Electrochemical Energy Reviews (2020) 3:370–394
https://doi.org/10.1007/s41918-020-00066-3

REVIEW ARTICLE

Recent Progress in Graphene-Based Nanostructured Electrocatalysts for Overall Water Splitting

Asad Ali[1] · **Pei Kang Shen**[1]

Received: 8 August 2019 / Revised: 5 October 2019 / Accepted: 5 November 2019 / Published online: 7 May 2020

Abstract
Graphene-based nanomaterials are promising bifunctional electrocatalysts for overall water splitting (OWS) to produce hydrogen and oxygen as sustainable fuel sources because graphene-based bifunctional electrocatalysts can provide distinct features such as large surface areas, more active sites and facile synthesis of multiple co-doped nanomaterials. Based on this, this review will present recent advancements in the development of various bifunctional graphene-based electrocatalysts for OWS reactions and discuss advancements in the tuning of electronic surface-active sites for the electrolytic splitting of water. In addition, this review will evaluate perspectives and challenges to provide a deep understanding of this emerging field.

Keywords Graphene · Electrocatalysts · Bifunctional · Overall water splitting

1 Introduction

Renewable and sustainable energy technologies are fundamental for future strategic development and economics in which hydrogen, possessing efficient, clean, global energy security and eco-friendly features, can play a significant role [1–5]. Based on this, water electrolysis has been broadly applied to produce pure hydrogen with zero carbon emission in the recent decade and is considered to be comparable to other sustainable sources (e.g., solar and wind) that produce electrical energy [6–9]. Here, the corresponding overall water splitting reaction (OWS) can be classified into two half electrochemical reactions including the oxygen evolution reaction (OER), which occurs at the anode and the hydrogen evolution reaction (HER), which occurs at the cathode [10–12]. The OWS reaction is a thermodynamically unfavorable process, however, at a theoretical voltage of 1.23 V and requires a thermodynamic Gibbs free energy of 237.2 kJ mol^{-1}. In addition, the HER (2-electron transfer) and OER (4-electron and proton) routes can kinetically generate energy fences and further impede OWS kinetics. Therefore, electrocatalysts are required to decrease kinetic energy barriers and increase HER and OER reaction kinetics [13]. And because most OWS reactions are studied in alkaline media, highly active HER electrocatalysts in alkaline solutions are vital [14].

In terms of electrocatalysts, their composition and the shape of supporting materials are essential aspects that can determine the performance and cost of the overall electrochemical process [4]. And although Pt/C electrodes as cathodes (HER) and IrO_2 electrodes as anodes (OER) can produce promising results, their exorbitant costs and low natural abundance severely hinder the widespread implementation of OWS. Therefore, alternative high-performance electrocatalysts and robust supporting materials for OWS are necessary to replace noble metal-based nanomaterials. Based on this, numerous electrocatalysts and supports have been designed to replace IrO_2 and Pt/C, including nanocarbon materials [15], carbon black [16], carbides [17], borides [18], oxides [19], nitrides [20] and polymers [21] to take advantage of their nature abundance and promising electrolytic performances [22–24].

And among these various materials, graphene-based materials including graphene as an electroactive component, reduced graphene, graphene quantum dots, doped graphene and functionalized graphene supports have shown particularly promise in water electrolytic applications (Scheme 1) [25, 26] and have gained much attention in the catalysis

✉ Pei Kang Shen
pkshen@gxu.edu.cn

[1] Collaborative Innovation Center of Sustainable Energy Materials, Guangxi Key Laboratory of Electrochemical Energy Materials, State Key Laboratory of Processing for Non-ferrous Metal and Featured Materials, Guangxi University, Nanning 530004, Guangxi, China

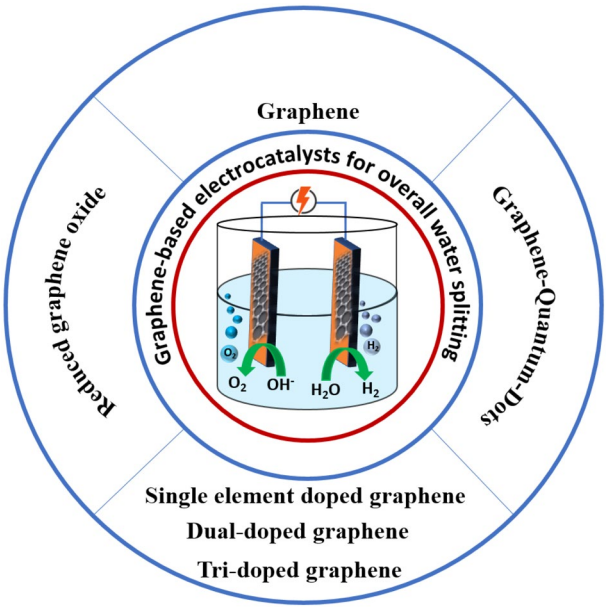

Scheme 1 Schematic of graphene-based electrocatalysts for overall water splitting

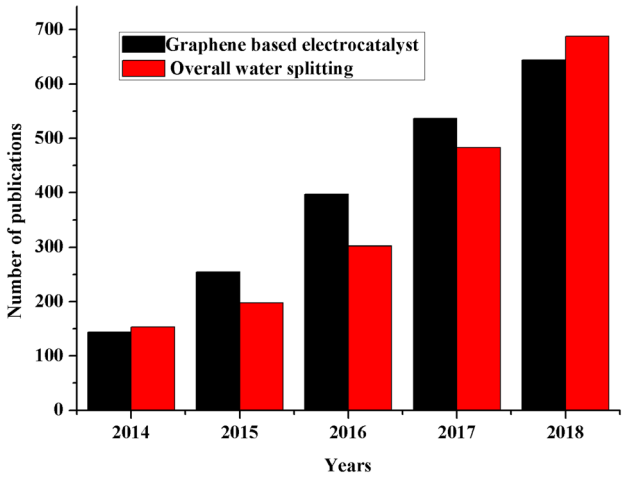

Fig. 1 Publications using graphene-based electrocatalysts and overall water splitting (numbers obtained from Web of Science)

field due to their intrinsic properties [27]. Graphene is a novel carbon material first discovered by Novoselov et al. [28] and has opened a new chapter in the development of materials science. Significantly, graphene is a two-dimensional hexagonal packed carbon atom nanosheet that possesses fascinating characteristics including superior electrical conductivity, remarkable mechanical strength and huge theoretical surface area (2630 $m^2 g^{-1}$) [29, 30]. In addition, graphene is composed of sp^2 carbon atoms bonded through three sigma (σ) bonds with adjacent carbon atoms [31] in which chemical doping can be used to tune electronic characteristics and alter reaction kinetics [32, 33]. As examples of graphene materials for OWS, hollow CoP nanomaterials loaded on N-doped graphene as a bifunctional electrocatalyst can reportedly show excellent performances at 1.58 V to reach a current density of 10 mA cm^{-2} and considerable durability for continuous 65 h of electrolysis as compared with commercial Pt/C [34], and metal-free N, F co-doped porous graphene nanosheet bifunctional electrocatalysts (NFPGNS) for OWS reactions can provide a lower onset voltage (1.60 V) that is slightly higher than commercial Pt/C electrocatalysts [35]. In addition, researchers have also reported that the compositional tuning and delicate nanostructuring of graphene-based electrocatalysts can further boost OWS performances [36]. And as a result of these promising conclusions, graphene-based electrocatalysts are gaining increasing application for OWS (Fig. 1).

As an emerging energy technology, many reviews have been published on OWS over the years [37–40]; however, a well-rounded review on graphene-based electrocatalysts for OWS is lacking. And considering the numerous publications, this review will highlight the recent advances and progress of graphene-based electrocatalytic applications toward OWS reactions and present mechanisms and applications of corresponding graphene-based electrocatalysts. In addition, this review will discuss improvement strategies for graphene-based electrocatalysts such as topological defect and edge engineering, interfacial and support effects and explore the OWS performances of various graphene-based materials, including graphene quantum dots, reduced graphene, single-doped graphene, dual-doped graphene and ternary-doped graphene-based electrocatalysts. Furthermore, this review will focus on various strategies and critical aspects to design high-performance graphene-based nanocatalysts and provide a look into the current progress and future perspective of graphene-based electrocatalysts along with critical challenges for this emerging topic.

Overall, this review will be an useful guide for the energy storage community to provide a practical framework for the future development of graphene-based electrocatalysts for OWS.

2 Graphene-Based Electrochemistry of Overall Water Splitting

The OWS reaction can be divided into two half-cell reactions including the oxygen evolution reaction (OER), which involves sluggish four-electron transfer at the anode [41–44] and the hydrogen evolution reaction (HER), which involves fairly facile two-electron transfer at the cathode [45–48]. And according to different pH solutions in which water splitting occurs, OWS can be chemically expressed as:

Overall water splitting: $2H_2O \rightarrow 2H_2 + O_2$

In alkaline media:

At anode: $4OH^- \rightarrow 2H_2O + O_2 + 4e^-$

At cathode: $2H_2O + 2e^- \rightarrow H_2 + 2OH^-$

In acidic media:

At anode: $2H_2O \rightarrow 4H^+ + O_2 + 4e^-$

At cathode: $4H^+ + 4e^- \rightarrow 2H_2$

Overall, most graphene-based electrocatalysts are functional in both acidic and alkaline media for HER, but are almost only functional in alkaline media for OER. Based on this, OWS in acidic environments require scarce, expensive, acid-insoluble and stable electrocatalysts. Regardless, both HER and OER electrocatalysts should be functional in the same electrolyte to allow for OWS reactions [49]. As for the thermodynamic voltage for OWS, this is 1.23 V at 1 atm and 25 °C [50–53] and the theoretical standard potentials for HER and OER are 0 and 1.23 V at 25 °C, respectively, in both acidic and alkaline media. Despite this, additional energy is required to overcome the overpotential induced by the activation barrier to initiate the initial reaction [54]. Here, the four-electron transfer mechanism of OER is kinetically sluggish, energy-intensive and complex in which bond formation occurs between oxygen atoms and bond breakage occurs between oxygen and hydrogen atoms [55] and electrocatalysts exhibiting lower overpotentials for OER can promote simultaneous OWS whereas electrocatalysts exhibiting high overpotentials for OER can impede OWS.

Overall, hydrogen adsorption potential is a prime factor in the design of HER catalysts whereas OH* adsorption capability to produce OOH* intermediates needs to be considered in the design of OER catalysts. In addition, N and S atoms can act as active sites in graphene-supported electrocatalysts in which electrolytic performances can be significantly improved through the synergistic effects of S and N-doping. Furthermore, morphological defects in graphene-based electrocatalysts as created through activation strategies can also significantly enhance OWS reactions [56]. For example, Boukhvalov et al. [57] reported that conventional OWS on activated graphene can proceed through a four-step mechanism (Fig. 2) involving: (1) H_2O reacts with activated graphene to generate graphene-OH and H^+ ions; (2) graphene-OH loses its H to generate graphene-O; (3) another H_2O reacts with graphene-O to generate H^+ ions and graphene-OOH; and ultimately, (4) graphene-OOH isolates from the activated graphene nanosheets to produce O_2 molecules and H^+ ions.

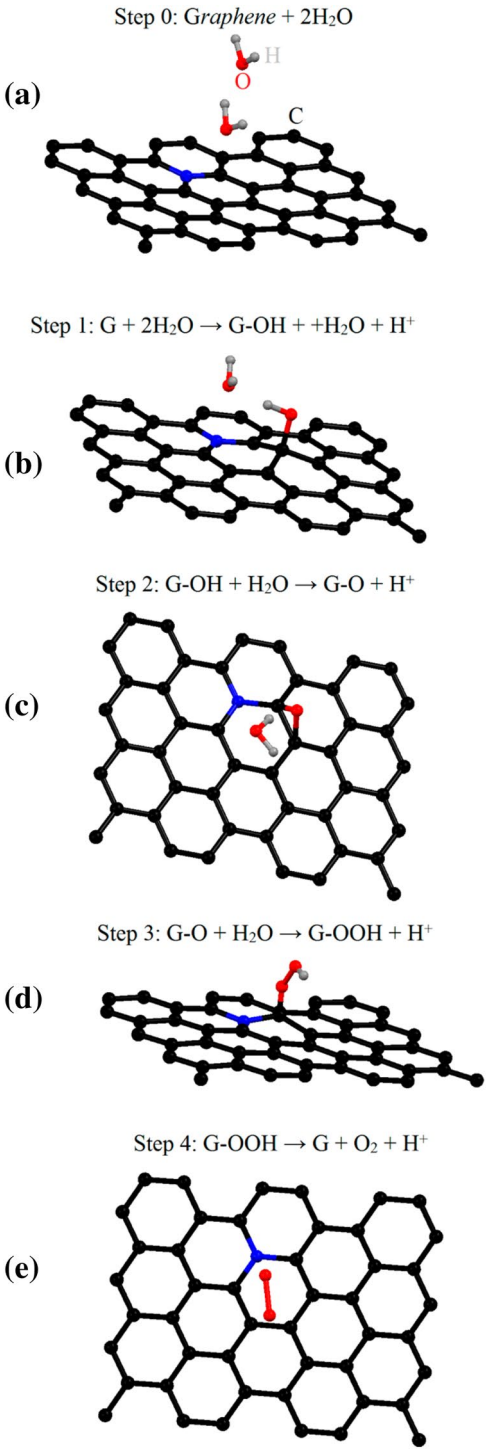

Fig. 2 Schematic of H_2O splitting on N-doped graphene. Reprinted with permission [57]. Copyright 2016 American Chemical Society

In another example, Gu et al. [58] reported that electrons from Ni_3FeN nanoparticles can transfer to reduced GO (rGO) nanosheets to allow for interfacial charge redistribution and that the aggregation of electrons on the rGO nanosheets can increase C–H bonding and promote HER

performance. In addition, these researchers reported that the transfer of electrons can affect overall agglomeration on Ni_3FeN nanoparticles to allow for optimal binding energies for intermediates and remarkable OER activities. Here, different intermediates possess different adsorption free energies on rGO-based electrocatalysts at zero potential (Fig. 3a) and the remarkable activity of the Ni_3FeN (111)/rGO electrocatalyst was demonstrated based on a calculated low overpotential of 0.46 eV. These researchers also reported that based on HER calculations, the potential of Fe_2N (001)/rGO and Ni_3N (001)/rGO electrocatalysts was 0.62 and 0.53 eV, respectively (Fig. 3b) whereas the ΔG_H* of the Ni_3FeN (111)/rGO electrocatalyst possessed the lowest potential of 0.17 eV.

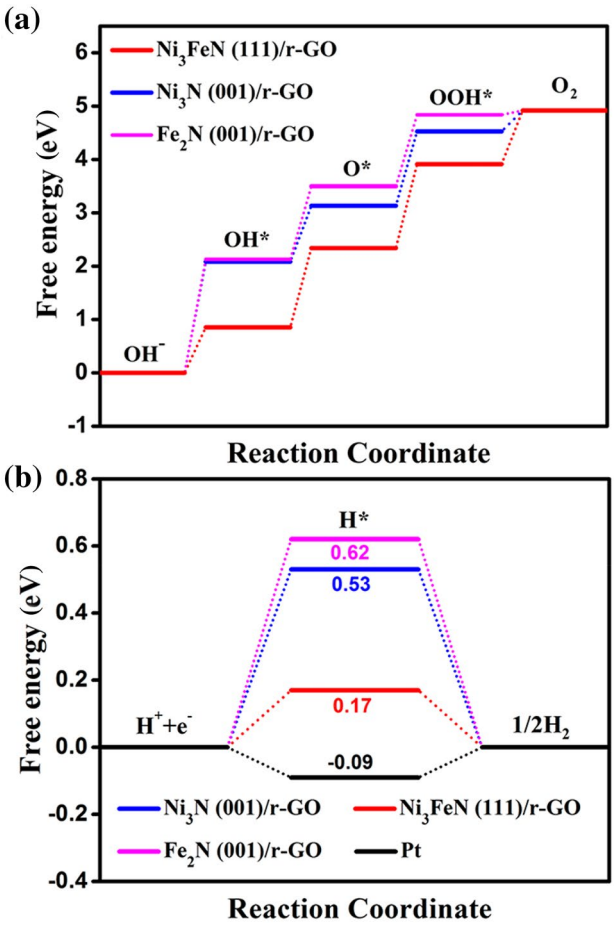

Fig. 3 Schematic of various free energy models for **a** OER and **b** HER. Reprinted with permission [58]. Copyright 2017 American Chemical Society

3 Strategies to Enhance Graphene-Based Electrocatalysts

The morphology of graphene-based electrocatalysts can significantly affect the OER and HER performance of OWS reactions. Here, interfacial atomic and surface engineering can be achieved by distorting graphene nanosheets either through the design of topological defects, heteroatom doping or through the creation of active edges, with every approach possessing distinct influences on OWS, both OER and HER. Overall, topological defects, active edges, interfaces and support effects are characteristics in graphene-based electrocatalysts that can be generated through chemical and physical strategies. And with the rapid development in theoretical studies, experimental methods and characterization approaches, deeper fundamental comprehensions of interfacial and support effects between supports and electrocatalysts can be obtained, leading to the large-scale synthesis of inexpensive and high-performance OWS electrocatalysts.

3.1 Topological Defect and Edge Engineering

The development of high-performance electrocatalysts through porosity design is a promising direction for OWS reactions [59], and recently, topological defect engineering has emerged as a promising strategy to increase the number of active sites in graphene-based catalysts [60–64]. Here, topological defects and active edges can directly act as active sites in graphene-based OWS electrocatalysts to impart anchoring sites for other vigorous nanomaterials (i.e., metals) [65] and the unique 2D planar morphology of graphene nanosheets can allow plane edges to strongly interact with nanoparticles. In addition, the growth of active nanoparticles on functional graphene surfaces is another promising strategy to promote electron conductivity and control nanoparticle morphology [38]. Moreover, edge engineering strategies to obtain graphene quantum dots and pores can also be used to increase the number of active edges in graphene and develop large surface area graphene-based electrocatalysts [66–71]. Overall, topological defects and active edges have two significant roles in graphene-based electrocatalysis, including: (1) directly acting as electroactive sites and (2) providing anchoring sites for other active components such as heteroatoms or metals.

One issue involving the active sites of graphene-based electrocatalysts is to increase the metal atoms confined at adsorption active sites such as graphene edges. To address this, Zhang et al. [72] reported that high-density defective graphene (DGN) can potentially contribute many effective

anchor edges through efficient charge promotion between the atoms of nanomaterials and the antibonding 2p state of graphene atoms to substantially increase the amount of metal nanomaterials on the surface of defective graphene. In another study, Chen et al. [73] found that the use of reduced graphene oxide (rGO) in synthesis can lead to the heteroepitaxial enlargement of Ni-ZIF nanoflakes on the surface of rGO sheets. Furthermore, Lu et al. [74] concluded that N-doped graphene (N-GN) morphology can contribute to significant surface defects and edges, which can enhance the number of active sites to promote electrolytic activity. And as a result, these researchers reported that the N-GN essentially prevented the agglomeration of active CoP nanoparticles, produced more active sites and correlated the CoP nanoparticles to enhance OWS performance, thus effectively increased the conductivity of the catalysts and promoted charge mobility between the electrolyte and electrocatalyst. Moreover, Yang et al. [75] reported that integrated Ni_3S_4 nanohybrids implanted in graphitic carbon nitride over N-doped graphene can prevent abscission, aggregation, irreversible mechanical failure and anisotropic volume expansion during electrolytic water splitting.

Overall, the modification of graphene morphology can promote the transfer of electrons from metal cores based on the binding energies of reaction intermediates. Here, graphene nanosheets possess weak adsorption potentials for intermediate H*, and electron transfer from metal cores to graphene can enhance C–H adsorption to promote HER performance [76]. For example, Li et al. [77] successfully synthesized Co and Ni-based nanoparticles on graphene nanosheets and found that their graphene/Ni hybrid was stable in alkaline media and can be used as a strong support for electrocatalysts in which its high electrical conductivity was beneficial for charge collection and transport, and its morphology offered open channels for electrolyte penetration to enhance OWS performance. Jia et al. [78] also reported that different morphological defects such as pentagons, heptagons and octagons with various combinations (i.e., 585 and 75585) can be observed close to lattice vacancies in defective graphene (DGN) (Fig. 4a) and found that structural defects were mostly found on hole edges in which hexagonal-shaped graphene nanosheets were dominant in the expanded parts of the electrocatalyst. Here, these researchers studied the structural evolution of GN → N-GN → DGN through atomic force microscopy (AFM) and found that the expulsion of N atoms can cause the demolition of graphene nanosheets (Fig. 4b).

Electrolytic active sites and edges of graphene-based electrocatalysts for OWS mainly exist on the surface of graphene, and researchers have reported that the coupling effect between the shell of N-doped graphene and Ni core can increase OER and HER performances. For example, Xu et al. [79] took advantage of the synergetic effects in a Ni/N-GN electrocatalyst and used N-doped graphene and Ni cores to tune surface morphology and increase OWS performance. Li et al. [80] also modified the shape of Mo@Ni_3S_2 microspheres to porous 3D stratified nanohybrids in the presence of GQDs to enhance the number of active edges and the conductivity of the close-packed Mo@Ni_3S_2/GQDs electrocatalyst. Furthermore, Zhao et al. [81] observed that the intimate contact between graphene and carbon quantum dots can allow for rapid charge transfer and halt carbon quantum dot agglomeration to impart remarkable electrocatalytic performance and durability. In addition, Zhao et al. [81] reported that the different defects/active edges on the surfaces of carbon quantum dots and graphene nanosheets as obtained through breaking and remaking during solvothermal synthesis can impart different electroactive edges for OWS reactions.

Jia et al. [82] also reported that the charge transfer between DGN and Ni–Fe-layered double hydroxide nanosheets (LDH-NS) can effectively enhance HER and OER based on DFT calculations and the geometries of the fully relaxed top view of Ni–Fe (LDH-NS)/DGN (DGN-5, DGN-585 and DGN-5775) as well as the differences of charge density (Fig. 5a, b). Here, these researchers reported that after assembling the DGN and Ni–Fe LDH-NS, electrons were redistributed around the defect sites and that electron transfer from Ni–Fe LDH-NS to graphene was observed

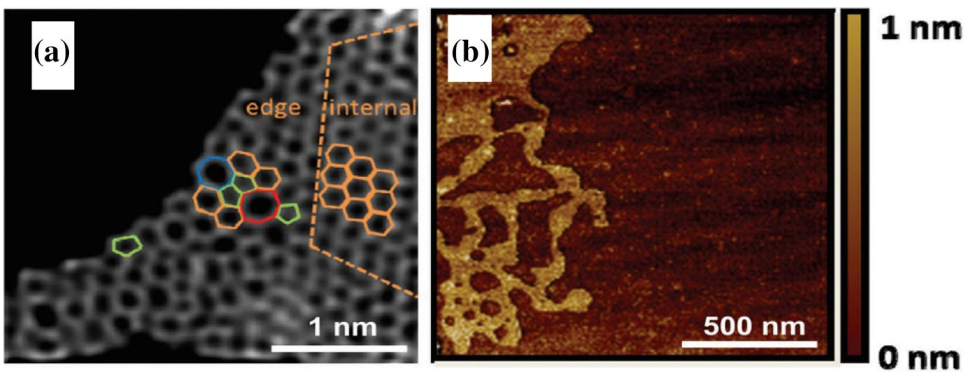

Fig. 4 **a** HAADF image of DGN (acceleration voltage = 80 kV). Orange, green, blue and red represent hexagons, pentagons, heptagons and octagons, respectively. **b** AFM image of DGN. Reprinted with permission [78]. Copyright 2016 John Wiley and Sons

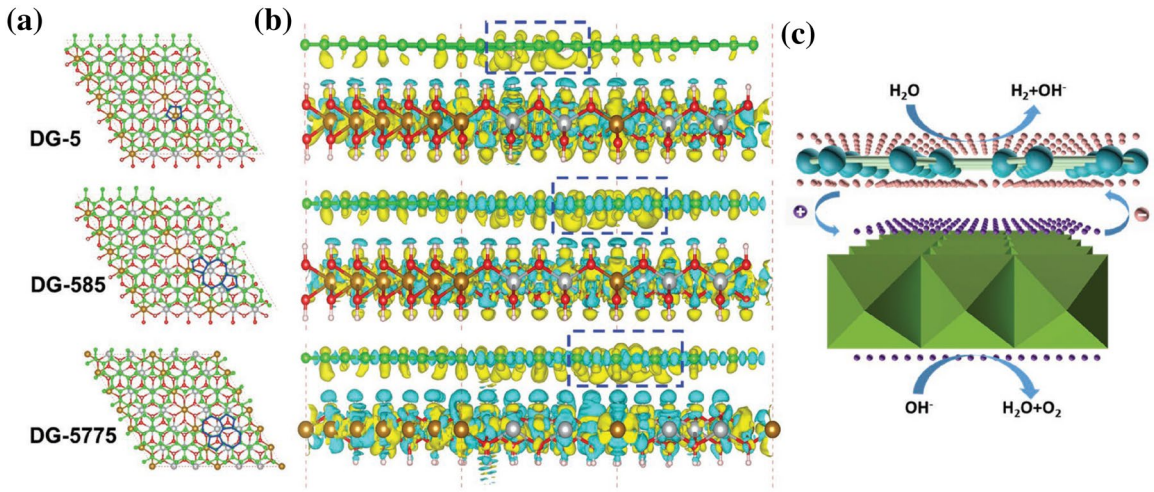

Fig. 5 DFT calculations of Ni–Fe (LDH-NS)/DGN (DGN-5, DGN-585 and DGN-7557). **a** Top interfacial views of optimized Ni–Fe (LDH-NS)/DGN (DGN-5, DGN-585 and DGN-5775). **b** Side views of the 3D charge density of the interfaces between DGN nanosheets (DGN-5, DGN-585 and DGN-5775) in which a Ni–Fe LDH-NS layer is exhibited. **c** Schematic of OWS using Ni–Fe (LDH-NS)/DGN for OER and HER based on DFT calculations. Reprinted with permission [82]. Copyright 2017 John Wiley and Sons

in the DGN but was negligible in GN and N-GN. Based on this, these researchers concluded that the nanocomposite of Ni–Fe LDH-NS and DGN can promote the redistribution of electrons and the separation of holes in which the high density of electrons on DGN can facilitate HER whereas the high density of holes on Ni–Fe LDH-NS can improve OER (Fig. 5c). In addition, these researchers reported that the high defect density of DGN can also provide more active sites in the NiFe LDH-NS@DGN catalyst to enhance HER/OER performances in which DGN can provide more efficient anchor sites to directly couple transition metal atoms (Ni and Fe) on the 2D exfoliated NiFe LDH nanolayers as compared with GN or N-GN. Moreover, these researchers also reported that the incorporation of DGN can prevent the aggregation of exfoliated LDH nanosheets to allow for an enlarged and stable electrochemical active surface area.

3.2 Interfacial Effects

Interfacial effect engineering in graphene-based electrocatalysts is a promising approach to develop low-cost, high-performance OWS electrocatalysts. Here, interfacial effects can arise from strong electronic interactions between two individual active constituents [83–86] in which active centers created at the interface can provide remarkable performances as compared with individual constituents. In addition, heterostructured graphene with abundant interfaces can exhibit remarkable chemisorption capabilities for both HER and OER to provide enhanced electrocatalytic performance and stability in alkaline electrolytes [13]. For example, Jayaramulu et al. [87] conducted the in situ solvothermal synthesis of hierarchical porous nanosheets of N-doped graphene oxide (N-GO) and nickel sulfide (Ni_7S_6) derived from a nickel-based metal–organic framework (NiMOF-74) using thiourea as the S source (Fig. 6 a–c) and reported that the N-GO/Ni_7S_6 hybrid demonstrated bifunctional performance for both HER and OER with remarkable stability in alkaline medium and attributed this to its tailored reaction interface, which can enhance the availability of electroactive nickel sites, mass transport and gas release.

In other examples, Ma et al. [88] reported that remarkable performances can be achieved from synergetic effects arising from the interfacial face-to-face hybridization of layered double hydroxide nanosheets and conductive graphene at a molecular level in a superlattice morphology and Li et al. [89] reported that the synthesis of NiFeP nanoparticles on strutted graphene (SG) can provide excellent distributions of NiFeP as well as reduced resistances between SG and NiFeP in which the porous morphology of SG can contribute to a substantial electrocatalyst-electrolyte interface as well as assist in the transport of electrons and H_2/O_2 liberation. In another study, Yuan et al. [90] reported that the constructed synergetic interface between N-graphene (N-GN) and exfoliated black phosphorus (EBP) can play a principal role in the increased OWS performance of the resulting EBP/N-GN. Here, these researchers reported that electrons withdrew from N-GN after EBP contact, which can lead to electrons enriching EBP active sites as confirmed by XPS analysis (Fig. 7a) in which the work function of EBP (4.7 eV) was higher as compared with N-GN (4.5 eV) and exhibited a lower Fermi level for EBP as further confirmed by Kelvin probe force microscopy (KPFM) (Fig. 7b). And because it is synergistically suitable for the migration of electrons from N-GN nanosheets to EBP following the redistribution of

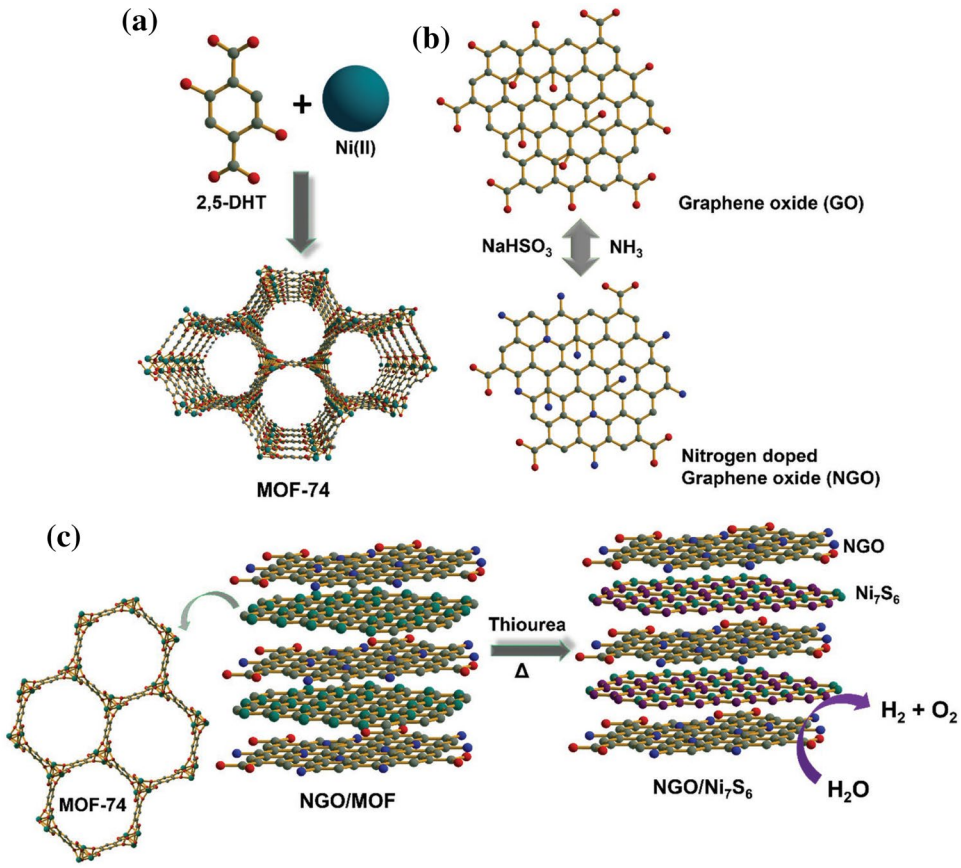

Fig. 6 **a** Schematic of the synthesis of NiMOF-74 using 2,5-dihydroxy terephthalate and Ni and **b** selective N-GO. **c** Schematic of the in situ synthesis of 2D N-GO and N-GO/Ni_7S_6. Reprinted with permission [87]. Copyright 2017 John Wiley and Sons

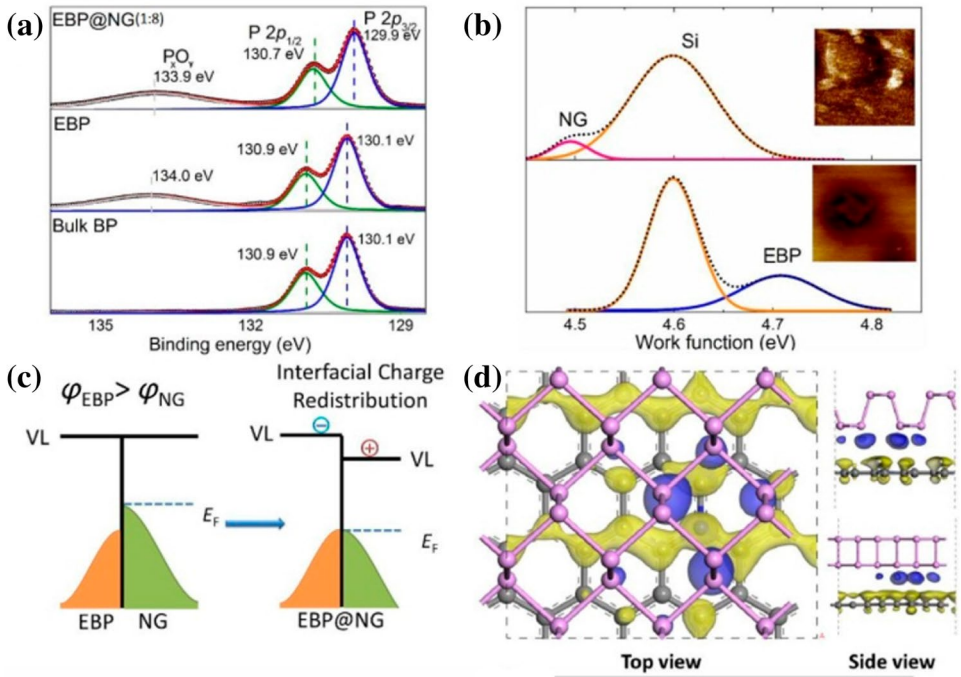

Fig. 7 **a** XPS spectra of bulk BP, EBP and EBP/N-GN. **b** Work function plots of EBP and N-GN. Insets show the results of Kelvin Probe Force Microscopy (KPFM). **c** Interfacial charge redistribution diagram between EPB and N-GN. **d** Charge densities of EPB and N-GN (blue and yellow surfaces represent high densities of electrons and holes, respectively). Reprinted with permission [90]. Copyright 2019 American Chemical Society

interfacial charge, high densities of electrons and holes can be achieved, respectively, for the calculated charge density of EBP@N-GN (Fig. 7c, d).

3.3 Support Effects

Aside from acting as electrocatalysts, graphene as porous supports has also attracted significant attention [91–97]. And due to the adhesion of gas bubbles on the surface of graphene-based electrodes, gaseous electrocatalysts operate on the solid–liquid–gas phase interface in which the triple track of electrons, ions and gases are imperative. Overall, desirable graphene-based porous supports are crucial to promote OWS reactions [98] and fundamental conditions include: (1) high surface areas for enhanced exchange currents and reaction interfaces; (2) intrinsic conductive porous networks for rapid electron and charge transport; (3) macroporous channels for facile electrolyte diffusion and gas release; (4) corrosion resistance and high stability to prevent the exposure of nanoparticles to harsh environments and corrosion and to synergistically boost intermediate adsorption; and (5) inexpensive, eco-friendly and lightweight, which are highly desired in aerospace-portable fuel cells.

As an example, Li et al. [89] fabricated NiFeP nanoparticles supported on strutted graphene (SG) through an easy hydrothermal method followed by phosphorization that was composed of 3D network graphene membranes (Fig. 8a–c) and reported that 3D SG can serve as a monolithic support to scaffold electrocatalytically active nanomaterials in which NiFe-layered double hydroxide (LDH) was directly synthesized on 3D SG to obtain a NiFe LDH/SG intermediate. Here, NiFe LDH nanosheets were located uniformly on the surface of SG (Fig. 8d) and after phosphorization, a black phosphide can be obtained in which all XRD diffraction peaks of the NiFeP/SG were similar to those of Ni_2P, indicating a single-phase Ni_xFe_yP rather than a mixture (Fig. 8e). In addition, these researchers also reported that the NiFeP nanosheets were able to preserve intimate integration on SG (Fig. 8f, g).

4 Overall Water Splitting

OWS is a promising technology that can be used for the massive production of H_2 and O_2 fuel and OWS as catalyzed by graphene-based electrocatalysts is a substantial topic of research in which simple and activated graphene can play key roles as both active constituents and functional supports. Here, these two-electrode systems are not only similar to ordinarily applicable electrocatalytic cells

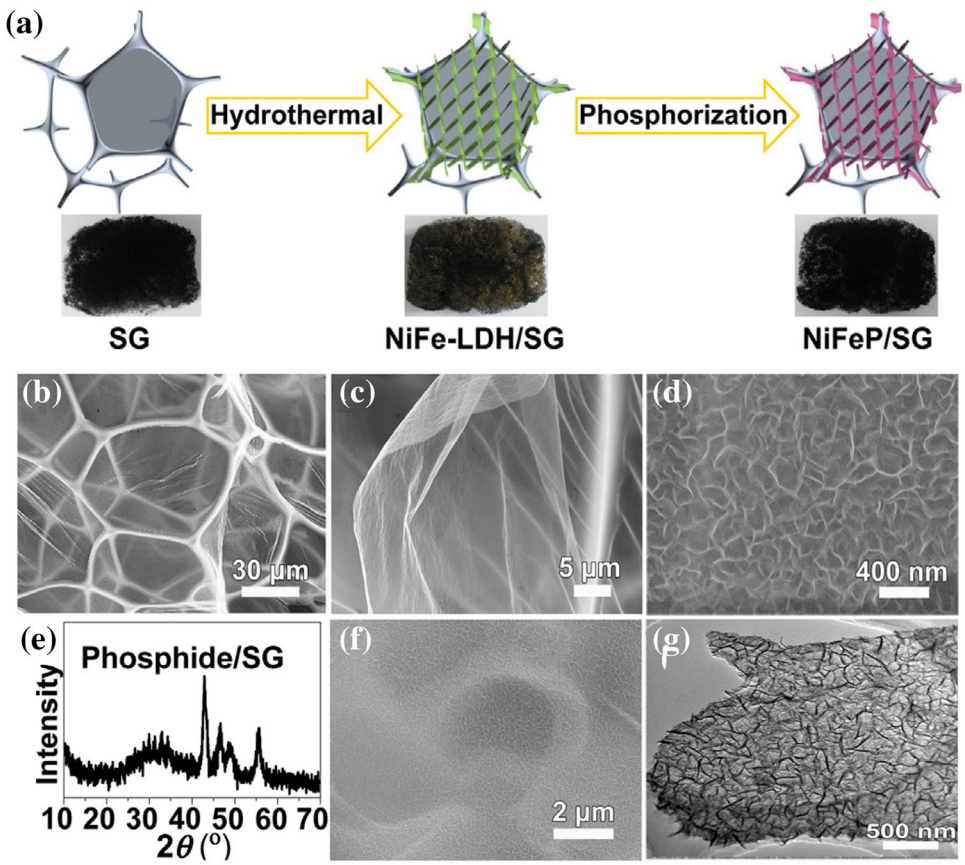

Fig. 8 **a** Schematic of a porous NiFeP/SG electrocatalyst. **b**, **c** SEM images exhibiting a 3D thin network of strutted graphene. **d** SEM image of NiFe LDH nanosheets on strutted graphene. **e** XRD pattern, **f** SEM image and **g** TEM image of a NiFeP/SG electrocatalyst. Reprinted with permission [89]. Copyright 2019 Elsevier

but can also avoid the costly utilization of Pt as a counter electrode in which basic requirements for these electrocatalysts include remarkable electrocatalytic performance and durability toward OER and HER simultaneously in the same solution. And taking into consideration the adsorption principle of gases on the surface of solid electrocatalysts, three essential routes exist, including electrons, ions and gases. Furthermore, porous graphene can act as crucial supporting materials to promote feasible OWS toward industrial production. Overall, graphene supports are inexpensive, highly stable and corrosion resistant. In addition, graphene supports possess excellent intrinsic conductivity for rapid electron transport, large surface areas for enhanced reaction interfaces and macroporous networks for electrolyte diffusion and gas production. Based on this, the study of OWS using graphene-based electrocatalysts with both remarkable HER and OER performances is attractive and recently, many graphene-based electrocatalysts have been synthesized that have exhibited benchmarking overpotentials at 10 mA cm^{-2} (Table 1). Furthermore, graphene-based electrocatalysts for OWS can be categorized by the type of graphene used, such as graphene, reduced graphene, graphene quantum dots and doped graphene, and this section will present a detailed discussion of their synthesis and corresponding OWS activities.

Table 1 Comparison of the OWS activities of graphene-based electrocatalysts

Electrocatalysts	Electrolyte (M KOH)	E^a (V)	HER[b] η-j (mV)	OER[c] η-j (mV)	Stability[d] (h)
NiQD@NC@rGO [73]	1.0	1.563-10	133-10	265-10	24
NiFeP/3D strutted GN [89]	1.0	1.54-10	115-10	218-10	40
CoP/vertical graphene nano-hills (VGNHs) [99]	1.0	1.63-10	93-10	300-10	24
$Mn_{0.6}Co_{0.4}P$-rGO [36]	1.0	1.55-10	54-10	250-10	24
Ni-MoxC/N-GN [100]	1.0	1.72-10	162-10	328-10	14
FeMnP/GN [101]	0.1	1.55-10	200-10	300-10	75
$CoS_{1.097}$/N-GN [102]	1.0	1.56-10	124-10	240-10	45
$(Co_{1-x}Ni_x)(S_{1-y}P_y)_2$/GN [103]	1.0	1.65-10	117-10	285-10	50
Ni_2P/rGO [104]	1.0	1.61-10	142-10	260-10	50
Ni_3S_2/NGQDs/Nickel Foam [105]	1.0	1.58-10	218-10	216-10	12
FeCoNi/GN [76]	1.0	1.68-10	149-10	288-10	10
NiCoP/rGO [106]	1.0	1.59-10	209-10	270-10	75
CoNPs/Co–N–S Tri-doped-GN [107]	1.0	1.88-10	366-10	337-10	7
CoP/N-GN [34]	1.0	1.58-10	130-10	210-10	65
CoP/rGO [55]	1.0	1.70-10	150-10	340-10	22
CoP_2/rGO [108]	1.0	1.56-10	88-10	300-10	2.5
FeNiP/P-GN [109]	1.0	1.58-10	173-10	229-10	10
N-doped graphene-coated Fe–Ni alloy encapsulated in N-doped carbon hollow nanobox [98]	1.0	1.701-10	201-10	270-10	10
NiSe/N-GN [110]	1.0	1.69-10	285-10	311-10	8
Ni_3FeN/rGO [58]	1.0	1.60-10	94-10	270-10	100
CoS_2@N-GN [111]	1.0	1.53-10	204-10	243-10	12
NiCoP/P-rGO [112]	1.0	1.56-10	106-10	281.3-10	10
GQDs-Mo-Ni_3S_2 [80]	1.0	1.58-10	68-10	326-20	50
Co_3O_4/N-GN [113]	1.0	1.63-10	191 (-10)	311-10	25
$Ni_2Co_2P_2$/GQDs [114]	1.0	1.61-10	119-100	400-100	10
Co–N co-doped graphene [115]	1.0	1.68-10	165-10	313-10	30
CoP@N,P co-doped mesoporous graphene [116]	1.0	1.58-10	151 (-10)	276-10	24
GQDs/$Co_{0.8}Ni_{0.2}P$ [25]	1.0	1.54-10	93-15	287-15	50
NiMnCo/rGO [117]	1.0	1.56-20	151-10	320-10	24

[a] E the cell voltage of a two-electrode system at a current density of j (mA cm^{-2}) in alkaline electrolytes

[b] η current density of j (mA cm^{-2}) in alkaline electrolytes for HER

[c] η current density of j (mA cm^{-2}) in alkaline electrolytes for OER

[d] Least checked stability of a two-electrode system at a current density of j (mA cm^{-2}) in alkaline electrolytes

4.1 Graphene

In general, intrinsic graphene is inactive toward OWS. However, graphene-based bifunctionally active electrocatalysts such as Ni_3S_2@GN [118], CQD/GN [81] can exhibit significant electrocatalytic activities toward OWS reactions and 3D graphene supports can stimulate the triple transportation of gases, ions and electrons to enhance the dispersal loading of active materials. And although the dispersion of nanoparticles on graphene through binders can deteriorate the intrinsic performance and durability of electrocatalysts due to binder detachment and contact resistance [89], ultrathin GN can allow for the uniform dispersion of active species and can inhibit the agglomeration of both GN nanosheets and active nanoparticles on GN surfaces [119]. In addition, carbon quantum dots (CQDs)/graphene composites are metal-free electrocatalysts that can show outstanding catalytic performances and durability for OWS in alkaline media as a result of the multiple defect sites exposed by small-sized graphene nanosheets, defect-rich CQDs, large active surface areas and rapid charge transfer [81].

Vertical graphene nano-hills (VGNHs) can also significantly enhance OWS performance and possess desirable characteristics such as robustness, multiple active edges, superaerophobicity and high conductivity. For example, Truong et al. [99] synthesized CoP flower-like nanostructures loaded on VGNHs as confirmed by low- and high-magnification SEM images (Fig. 9a, b) and reported the bifunctional activity of the CoP/VGNHs electrocatalyst for OWS in 1.0 M KOH solution in which a current density

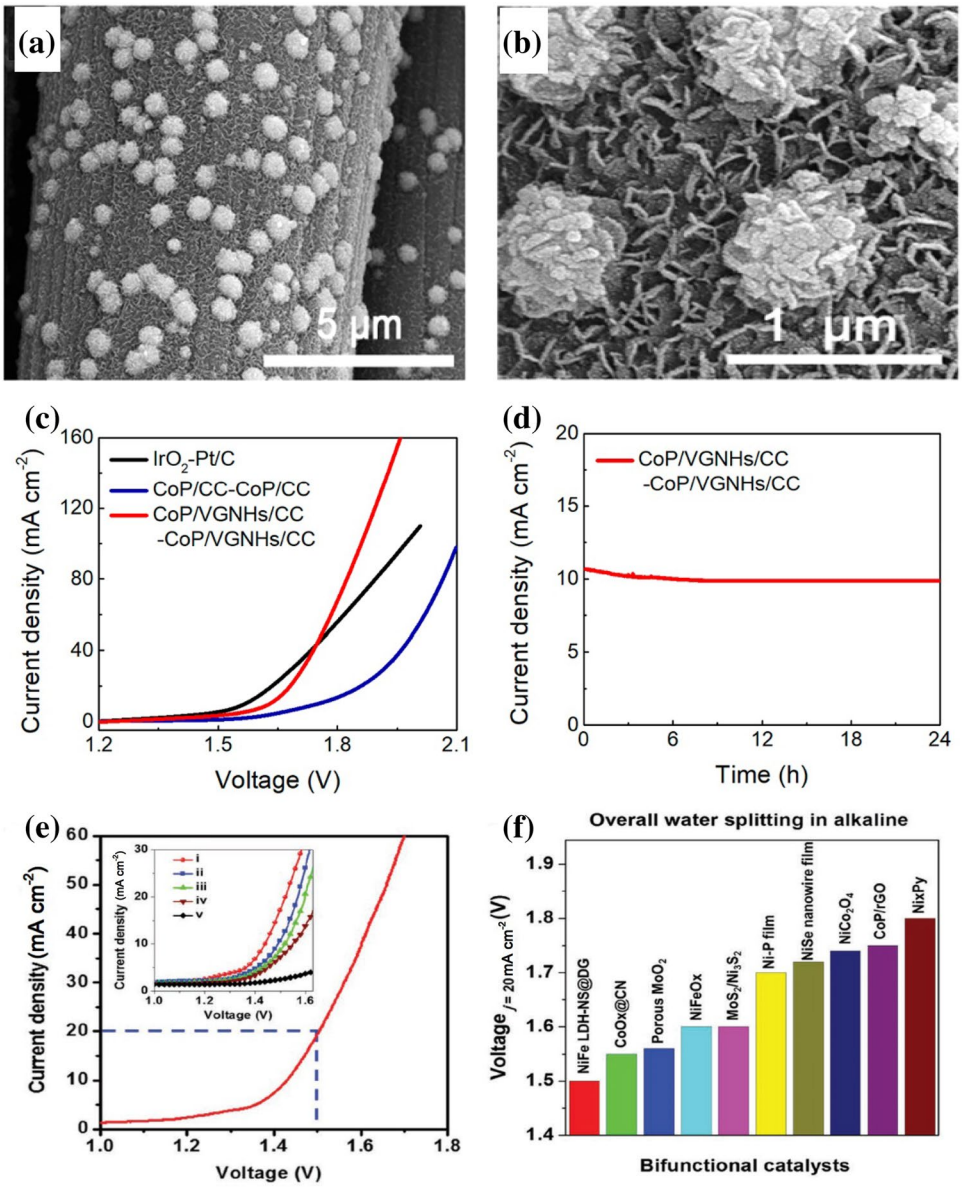

Fig. 9 **a** Low- and **b** high-magnification SEM images of CoP/VGNHs. **c** OWS in 1.0 M KOH solution. **d** Excellent stability of CoP/VGNHs at 1.63 V for 24 h using two water electrolyzers. Reprinted with permission [99]. Copyright 2019 American Chemical Society. **e** Linear sweeping voltammetry curves of NiFe LDH-NS@DGN as a HER and OER bifunctional electrocatalyst in 1.0 M KOH for OWS (inset shows the comparison between various electrocatalysts including (i) NiFe LDH-NS@DGN with 2 mg cm^{-2} loading; (ii) NiFe LDH-NS@DGN with 1 mg cm^{-2} loading; (iii) NiFe LDH-NS@N-GN with 2 mg cm^{-2} loading; (iv) NiFe LDH-NS@G10 with 2 mg cm^{-2} loading; and (v) a bare Ni foam electrode. (f) Voltage comparison at a current density of 20 mA cm^{-2} for the NiFe LDH-NS@DGN electrocatalyst with other bifunctional electrocatalysts. Reprinted with permission [82]. Copyright 2017 John Wiley and Sons

of 10 mA cm^{-2} at 1.63 V was achieved (Fig. 9c). These researchers also reported that the OWS reaction was highly stable as a result of the structural and chemical stability of the VGNHs support (Fig. 9d).

Jia et al. [82] in their study also reported that the OWS performance of a NiFe LDH-NS@DGN bifunctional catalyst can exhibit superior electrolytic rates as compared with NiFe LDH-NS@GN, N-GN and GN electrocatalysts (Fig. 9e) and that higher loadings of NiFe LDH-NS@DGN (2 mg cm^{-2}) can provide better OWS activities with a current density of 20 mA cm^{-2} at 1.5 V being achievable (Fig. 9e, inset), which is the best performance as compared with other non-noble metal bifunctional electrocatalysts for OWS in alkaline media (Fig. 9f). In addition, Xu et al. [120] reported that $(NiCo)Se_2$ nanocages dispersed on 3D graphene aerogels (GA) only required a low voltage of 1.60 V and exhibited remarkable durability and suggested that the 3D graphene nanosheets with abundant open spaces can promote charge transfer during electrocatalysis, resulting in a calculated experimental Faradaic efficiency of 97% as compared with theoretical O_2/H_2 production. In another study, Hou et al. [121] obtained a 3D electrocatalyst using an in situ strategy in which cobalt selenide ($Co_{0.85}Se$) was vertically dispersed on electroactive exfoliated graphene followed by a dispersion of NiFe-layered double hydroxide (LDH) through a hydrothermal process and reported that the obtained 3D electrocatalyst exhibited a current density of 20 mA cm^{-2} at 1.71 V for OWS reactions. Moreover, Li et al. [89] synthesized a 3D electrocatalyst by loading NiFeP onto 3D-strutted graphene (SGN) and reported that the synergetic effect between the 3D SGN network and NiFeP in the NiFeP/SGN electrocatalyst allowed for excellent OWS performances in alkaline media.

4.2 Graphene Quantum Dots

GQDs are an important member of the graphene family and can exhibit remarkable performances toward OWS reactions. In hybrid electrocatalysts, GQDs with other active materials can allow for increased interspacing and defects to enhance electrocatalysis and enable many mechanisms for electron and ion transfer. In addition, GQDs with its 0D planar shape can alter material morphology for the synthesis of different nanocomposites and the less than 2nm diameter of GQDs allows for higher specific surface areas as compared with other carbon nanomaterials. Interestingly, more functional groups can also be loaded onto the surface of GQDs and can increase wettability in water electrolysis. Furthermore, GQDs can be doped by many heteroatoms such as N, P and S to improve catalytic features. And in terms of facile synthesis methods, GQDs can also provide promising opportunities to design novel electrocatalysts for OWS reactions [80].

For example, Tam et al. [2] synthesized a novel electrocatalyst through a facile one-step hydrothermal strategy involving B-doped GQDs loaded onto graphene hydrogel (GH) (Fig. 10a) and reported that the BGQD-GH electrocatalyst possessed distinctive 3D morphology with a large specific surface area and many pores, thus allowing for abundant electrocatalytic active sites. As a result, the BGQD-GH electrocatalyst showed excellent bifunctional electrocatalytic performances toward OWS reactions with a long-term durability comparable to commercial Ir/C and Pt/C electrocatalysts. These researchers also reported that their BGQD-GH electrocatalyst used in a water splitting electrolyzer was able to provide a benchmark current density of 10 mA cm^{-2} at 1.61 V with extraordinary durability for at least 70 h without clear decay. In another example, Lv et al. [105] fabricated a noble metal-free hybrid through the in situ synthesis of N-doped GQDs (NGQDs) and Ni_3S_2 sheets on Ni foam and reported that the synergistic effect of the active interfaces was a key feature for the observed remarkable activity, allowing this hybrid to serve as an active, binder-free OWS electrocatalyst. Moreover, Cirone et al. [122] reported that GQDs can be used as a precursor for the synthesis of other nanomaterials to act as electrocatalysts for OWS reactions in which GQDs possess almost the same characteristics of graphene such as excellent electrical conductivity and stability. Furthermore, Tian et al. [114] studied bifunctional catalysts of nickel–cobalt phosphide ($NiCo_2P_2$) and GQDs for OWS in alkaline media (Fig. 10b) and encouraged by remarkable HER and OER activities, further explored a $NiCo_2P_2$/GQDs hybrid on Ti mesh as a bifunctional electrocatalyst in an alkaline electrolyzer (Fig. 10c). Here, these researchers reported that the $NiCo_2P_2$/GQDs hybrid was able to exhibit excellent OWS performances to achieve 10 mA cm^{-2} at a voltage of 1.61 V (Fig. 10d) and remarkable stability in which a constant current density of 10 mA cm^{-2} at an applied voltage of 1.61 V was maintained for 10 h with bubbles being observed at both electrodes (Fig. 10e). On the basis of well-dispersed GQDs, more active surface sites, fast electron transfer capabilities and the confinement effect, Hou et al. [25] also used GQDs/$Co_{0.8}Ni_{0.2}P$ tubular arrays as a cathode and anode and reported remarkable HER and OER activities in which the bifunctionally active GQDs/$Co_{0.8}Ni_{0.2}P$ composite displayed outstanding electrocatalytic activities for OWS with a current density of 10 mA cm^{-2} at 1.54 V and optimal operation stabilities in an alkaline medium.

Overall, the atomic structures, electronic structures and electrochemical features of GQDs are key to their mechanistic role in morphology control and enhanced performance. As a result, GQDs can encourage the synthesis of nanosheet-shaped electrocatalysts, which are better than nanowires or other nanostructures in terms of ion diffusion, charge transfer and active site exposure [114].

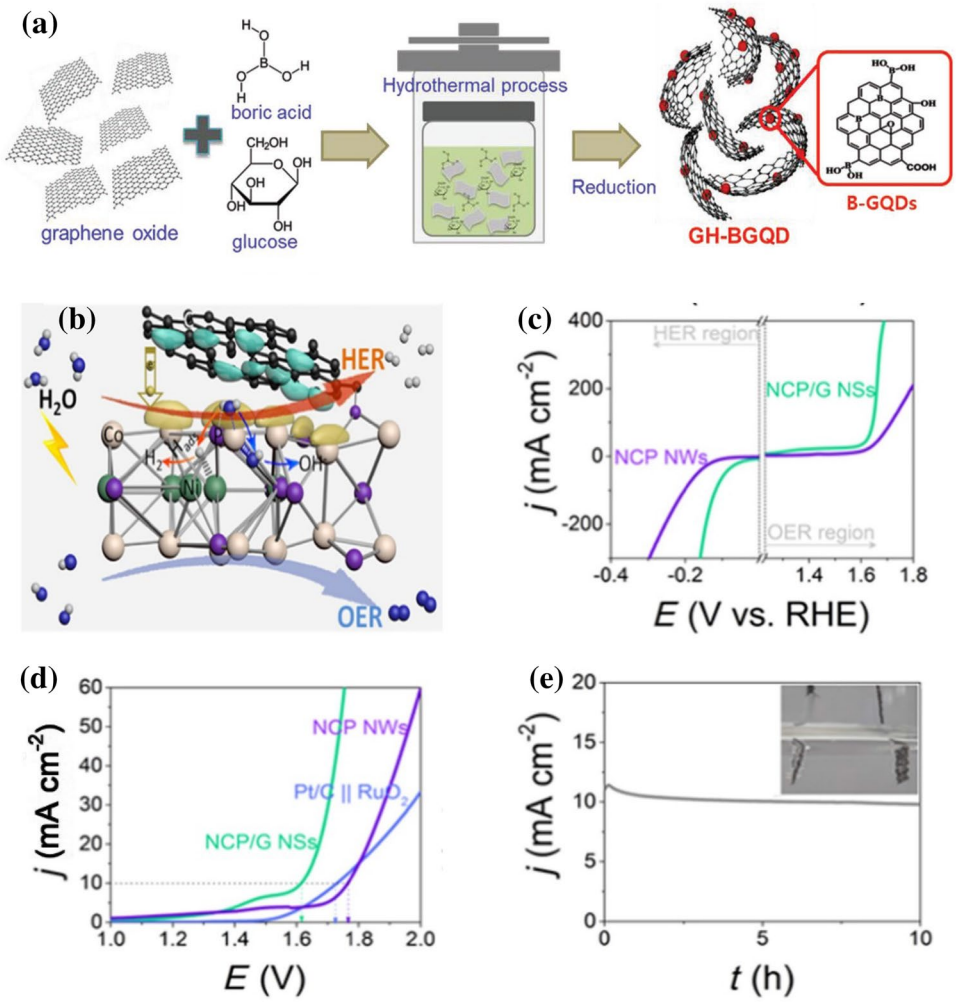

Fig. 10 **a** Schematic of the facile one-step hydrothermal synthesis of a BGQDs-GH electrocatalyst. Reprinted with permission [2]. Copyright 2019 John Wiley and Sons. **b** Schematic of the OWS mechanism for $NiCo_2P_2$/GQDs. Yellow and blue zones represent electron accumulation and depletion, respectively. **c** Polarization curves of $NiCo_2P_2$ nanowires (NWs) and $NiCo_2P_2$/GQDs at 2 mV s^{-1} in 1.0 M KOH. **d** Two-electrode polarization curves of $NiCo_2P_2$/GQDs, $NiCo_2P_2$ NWs and RuO_2 electrocatalysts. **e** Current density curve for $NiCo_2P_2$/GQDs || $NiCo_2P_2$/GQDs at 1.61 V for 10 h. Inset exhibits generated H_2 and O_2. Reprinted with permission [114]. Copyright 2018 Elsevier

4.3 Reduced Graphene Oxide

The reduction of graphene oxide (GO) to reduced graphene oxide (rGO) can reduce the average dimension of sp^2 domains and develop active edges in graphene surfaces that can act as defects in electrocatalysts [123]. In addition, the presence of rGO in electrocatalysts can further enhance electrocatalytic performances by influencing reaction kinetics and electron transport during OWS reactions [124]. And based on synergetic effects, reduced graphene-based electrocatalysts such as Ni QD@NC@rGO [73], Ni/rGO [125] and $Ni_{2/3}Fe_{1/3}$-rGO [88], etc. can exhibit significant OWS electrocatalytic activities. For example, Xu et al. [36] evenly loaded $Mn_{0.6}Co_{0.4}P$ nanoparticles onto rGO nanosheets after thermal conversion and suggested that the strong binding between rGO and $Mn_{0.6}Co_{0.4}P$ nanoparticles can strengthen interfacial association and avert $Mn_{0.6}Co_{0.4}P$ geometrical collapse and agglomeration during OWS to enhance stability in which these researchers reported that $Mn_{0.6}Co_{0.4}P$ nanoparticles without rGO support were found to be more agglomerated. Debata et al. [126] also synthesized bifunctional coral-shaped $NiCo_2O_4$ nanoparticles anchored onto rGO nanosheets through an easy hydrothermal method and reported high current densities, low onset potentials, lower Tafel slopes and good stability for both OER and HER, and Miao et al. [117] synthesized Ni, Mn and Co nanoparticles supported on rGO with further conversion to a spinel ternary sulfide through gaseous sulfurization. Here, these researchers reported that the OWS reaction in alkaline media of a water electrolyzer using a ternary oxide NiMnCo/rGO composite as the OER electrocatalyst and an as-converted ternary sulfide NiMnCo/rGO composite as the HER electrocatalyst (Fig. 11a) required a cell voltage of 1.56 V to obtain a current density of 20 mA cm^{-2} at room temperature (Fig. 11a, b). Moreover, Li et al. [106] synthesized a NiCoP/rGO for OWS and achieved a benchmark current density of 10 mA cm^{-2} at 1.59 V in 1.0 M KOH (Fig. 11c). Here, produced O_2 and H_2 was quantitatively measured by gas chromatography and matched with the theoretically calculated amount in which the molar ratio of O_2 and H_2 was near 0.5, thus showing 100% Faradic efficiency

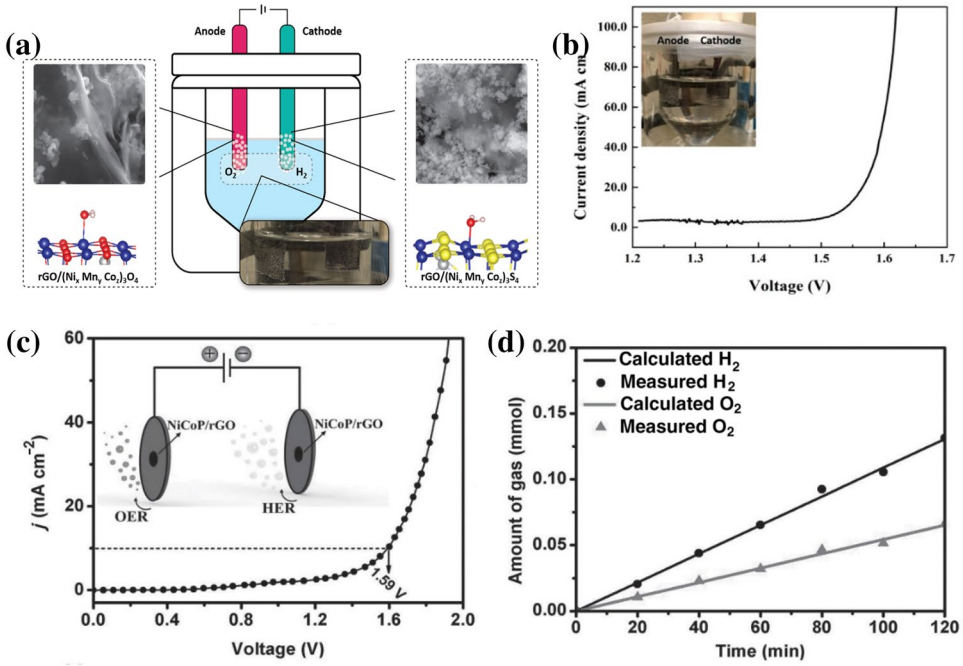

Fig. 11 **a** Schematic of OWS. **b** Polarization curve of OWS using NiMnCo/rGO ternary oxide nanocomposites as an anode and as-converted NiMnCo/rGO ternary sulfide nanocomposites as a cathode in 1.0 M KOH. Inset exhibits bubbles of H_2 and O_2. Reprinted with permission [117]. Copyright 2017 American Chemical Society. **c** The OWS activity of the NiCoP/rGO composite. Inset shows the schematic for the OWS reaction. **d** Comparison of O_2 and H_2 based on theoretically and experimentally measured gases versus time for OWS reactions using NiCoP/rGO composites at a current density of 25 mA cm^{-2}. Reprinted with permission [106]. Copyright 2016 John Wiley and Sons

(Fig. 11d) and demonstrating the excellent durability of the NiCoP/rGO electrocatalyst toward OWS reactions in alkaline media.

4.4 Doped Graphene

Overall, experimental and theoretical studies have shown that active sites play a crucial role in the overall performance of heterogeneous electrocatalysts and the generation of increased active sites on graphene electrocatalysts and the promotion of active site reactivity are essential approaches to increase electrocatalytic activity. Here, the incorporation of other elements can allow for more variations in atomic arrangement with more promising electron structures. Based on this, the doping of nanostructured graphene with heteroatoms such as B, F, N, S, P or O can allow for electron modulation and the tuning of electrochemical features [127–129] in which N-doping has shown particular promise. In addition, the heteroatom doping of graphene can result in distinct electronic structures and intensified electrochemical features due to the modification of electronic properties to decrease kinetic barriers. Furthermore, single, dual and triple doping have all been shown to increase the performance of graphene toward OWS.

4.4.1 Single-Element Doped Graphene

4.4.1.1 Nitrogen-Doped Graphene Based on synergetic effects, N-doped graphene-based electrocatalysts such as CoP@N-GN [74], Co_3O_4/N-GN [113] or $FeNi_3N$/N-GN [130] can exhibit significant electrocatalytic activities toward OWS. This is because the presence of N-doped graphene supports can prevent agglomeration and nanoparticle detachment during pyrolysis and thus help to maintain the morphological integrity of nanocomposites. In addition, N-doped graphene supports can prevent corrosion and overall structural collapse in alkaline media during OWS to provide excellent interactions between nanoparticles and alkaline media by promoting mass and charge transfer. Furthermore, N-doping for graphene can enhance electron density on graphene surfaces to allow for outstanding HER [100] and synergistically boost intermediate adsorption and enhanced OWS performance. Moreover, N-doped graphene nanosheets can enable electronic contact with vicinal nanoparticles and create structural defects on the surface of graphene nanosheets to increase active sites and therefore electrocatalytic performance [98]. For example, Liang et al. [102] reported that N-doped graphene can effectively prevent the aggregation of $CoS_{1.097}$ nanoparticles and therefore significantly enhance the contact area of $CoS_{1.097}$ nanoparticles with electrolytic solution. These researchers further reported that N-doping can minimize the function of graphene to enhance intermediate adsorption on graphene nanosheets and decrease the binding energy between the electrocatalyst surface and reaction intermediates to enable the N-doped graphene to be more reactive. In addition, these researchers also reported that the synergistic contact between $CoS_{1.097}$ nanoparticles and N-doped graphene can enhance OWS. In another study, Zhang et al. [131] reported that the synergism, hybridization and more active sites of N-doped rGO in a NiCoP/N-rGO composite provided better OER performances as compared with RuO_2 electrocatalysts

in alkaline media as well as enhanced electroactive HER in neutral, acidic and alkaline media in which their NiCoP/N-rGO showed remarkable electrochemical activities at a cell voltage of 1.57 V with a current density of 20 mA cm^{-2} for OWS. Zhang et al. [98] also reported that the distinctive morphology of N-doped graphene nanosheet-coated binary FeNi nanoparticles enclosed in a N-doped carbon hollow nanobox can provide multiple advantages as a bifunctional electrocatalyst for OWS, including low overpotentials of 201 mV (HER), 270 mV (OER) and 471 mV (OWS) with 10 mA cm^{-2} in 1.0 M KOH solution. Furthermore, Hu et al. [132] reported that their NiFe@MoC_2/N-GN electrocatalyst displayed excellent OWS performances and attributed this to the high stability and conductivity of N-doped graphene in which the NiFe@MoC_2/N-GN electrocatalyst only required a low cell voltage of 1.53 V to reach a current density of 10 mA cm^{-2} for OWS. Moreover, Kuang et al. [9] synthesized bimetallic sulfide nanoparticles loaded on 3D N-doped graphene foam (MoS_2-NiS_2@N-GF) as a bifunctional electrocatalyst in alkaline media for OWS in which N-GF was first prepared through a template-assisted approach by burning GO-absorbed melamine sponge (ca. 1 cm × 1 cm × 0.5 cm, consisting of C, H, N and O elements) (Fig. 12). And based on the synergistic effects of the N-GF and bimetallic sulfides as well as the novel 3D interconnected tubular morphology, the obtained MoS_2-NiS_2@N-GF possessed not only multiple active sites, but also diversified roots for the rapid and efficient transport of electrons and mass. As a result, these researchers reported that the MoS_2-NiS_2@N-GF delivered a current density of 10 mA cm^{-2} at an overpotential of 172 mV for HER and 370 mV for OER in 1.0 M KOH on a simple glassy carbon electrode. And if used in an alkaline water electrolyzer, the non-precious-metal MoS_2-NiS_2@N-GF on Ni foam produced vigorous and continuous evolution of H_2 and O_2 at a current density of 10 mA cm^{-2} under a cell voltage of 1.64 V, demonstrating that MoS_2-NiS_2 anchored onto 3D N-GF with its remarkable bifunctional performance is a promising candidate for cost-efficient and large-scale hydrogen production through OWS.

In terms of Ni@N-GN electrocatalysts, Xu et al. [79] reported that SEM images (Fig. 13a) revealed many sphere-shaped nanostructures 20–30 nm in diameters and high-resolution transmission electron microscopy (HRTEM) images confirmed that these spherical nanostructures were comprised of Ni nanoparticle cores that were encapsulated by a hollow shell composed of many graphene nanosheets in which the crystal plane of 0.21 nm *d*-spacing (Fig. 13b) corresponded to the (111) lattice of Ni nanoparticles and was encapsulated by a graphene shell 3–5 layers thick and 0.34 nm interlayer distance. And as a result, the linear sweep voltammogram (LSV) of OWS on the Ni@N-GN-800/Ni foam electrocatalyst in 1.0 M KOH solution (Fig. 13c) revealed that the Ni@N-GN/Ni foam electrode can provide excellent performances in which a current density of 10 mA cm^{-2} at 1.60 V for OWS can be obtained. In addition, these researchers also reported that the chronoamperometry curve at a cell voltage of 1.62 V demonstrated that the OWS activity of the Ni@N-GN/Ni foam was durable for 50 h and that O_2 and H_2 bubbles were produced (Fig. 13d). Aside from these results, researchers have also reported that the promising properties of porous carbon polyhedron (PCP), N and Co-doping effects, the inclusion of N-rGO and the tremendous interaction between N-rGO and N/Co-PCP can all allow for remarkable electrocatalytic performances [133]. For example, Zhang et al. [134] reported that a Co@CoO/N-GN electrocatalyst for OWS can achieve a current density of 10 mA cm^{-2} at the potential of 1.58 V and that Co@CoO core–shell nanoparticles supported on N-doped graphene was an active and durable bifunctional OWS electrocatalyst with activities comparable to those of Pt and IrO_2 electrocatalysts (Fig. 13e, f).

4.4.1.2 Phosphorous-Doped Graphene P is an important member of the N family and possesses the same number of valance electrons as N and similar chemical characteristics [135]. Based on this, Yang et al. [136] synthesized mixed-phase CoP-Co_2P@P-C/P-GN, Co_2P@P-C/P-GN and CoP@P-C/P-GN electrocatalysts by controlling the thermal conversion of as-prepared supramolecular gels containing graphene oxide, cobalt salt and phytic acid at optimal temperatures under Ar/H_2 environment (Fig. 14a) and reported that the CoP-Co_2P@P-C/P-GN electrocatalyst presented

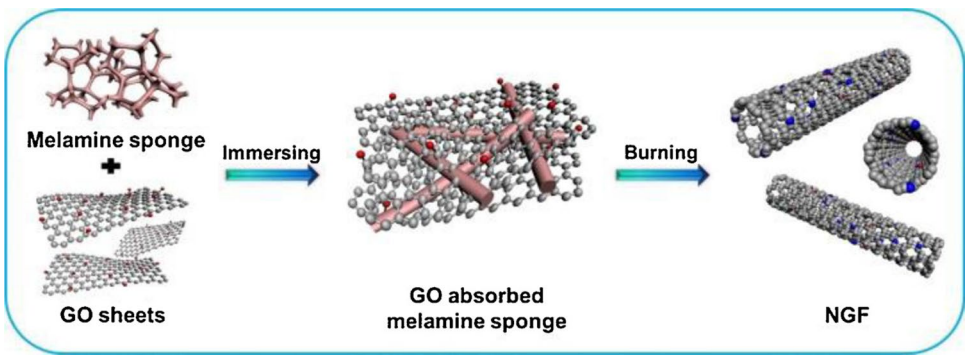

Fig. 12 Schematic for the synthesis of N-doped graphene foam (N-GF). Reprinted with permission [9]. Copyright 2019 Elsevier

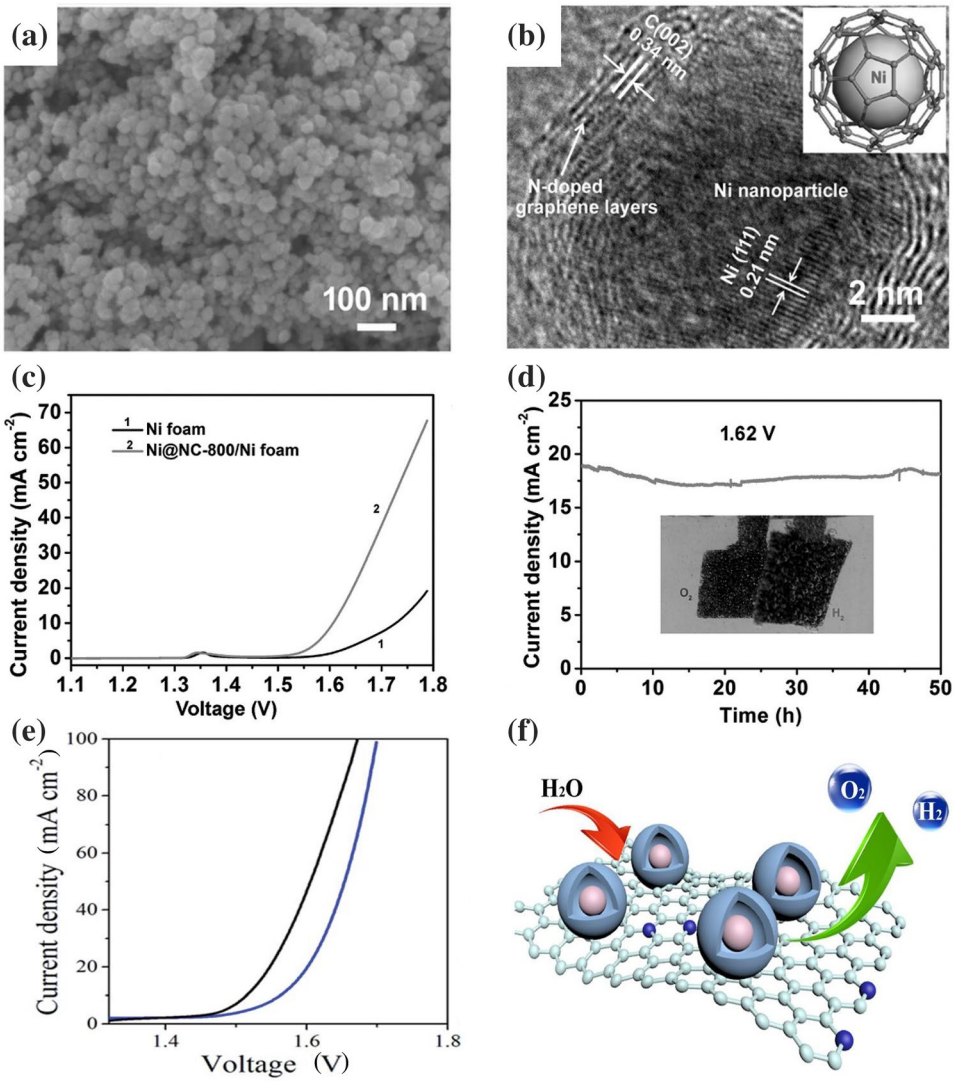

Fig. 13 **a** SEM and **b** HRTEM images of Ni@N-GN. Inset in b is a structural schematic of the Ni@N-GN electrocatalyst. **c** LSV curves of OWS using Ni@NC-800/Ni foam electrode as both the anode and cathode at 5 mV s^{-1} in 1.0 M KOH. **d** Chronoamperometry curve at a voltage of 1.62 V. (Electrocatalyst loaded on Ni foam: 0.8 mg cm^{-2}). Reprinted with permission [79]. Copyright 2017 John Wiley and Sons. **e** Polarization curves of Co@CoO/N-GN and IrO_2|Pt for OWS in 1.0 M KOH at 5 mV s^{-1}. **f** Schematic OWS representation of Co@CoO/N-GN electrocatalyst. Reprinted with permission [134]. Copyright 2016 Royal Society of Chemistry

excellent bifunctional OWS performances to deliver a HER overpotential of 39 mV at a current density of 10 mA cm^{-2} and an OER overpotential of 272 mV at a current density of 20 mA cm^{-2}. Here, a corresponding cell only required 1.567 V for OWS to obtain a current density of 10 mA cm^{-2} (Fig. 14b) and ran for over 30 h with negligible decreases in performance, thus demonstrating outstanding stability (Fig. 14c). Dong et al. [112] also encapsulated Ni–Co phosphide (NiCoP) in P-doped rGO nanosheets (P-rGO) and reported promising HER and OER activities in 1.0 M KOH electrolyte in which the NiCoP/P-rGO electrocatalyst exhibited remarkable OWS performances and durability and achieved a current density of 10 mA cm^{-2} at a cell voltage of 1.56 V. In addition, Bu et al. [109] reported that bimetal FeNi phosphide anchored on P-doped graphene can provide low overpotentials of 173 and 229 mV at a current density of 10 mA cm^{-2} in alkaline media for HER and OER, respectively, and that as used as both the anode and cathode, the FeNiP/P-graphene allowed for current densities of 10 mA cm^{-2} at 1.58 V and 50 mA cm^{-2} at 1.74 V, respectively, for OWS.

4.4.2 Dual-Doped Graphene

In terms of doping technologies, the synthesis of co-doped graphene with two different elements has recently been extensively explored by researchers [137–139]. This is because based on synergetic effects, dual-element doped graphene-based electrocatalysts can exhibit significant electrocatalytic activities toward OWS in which the rational composite of dual-doped graphene can provide enhanced activities as compared with single-doped graphene for OWS. And to date, multiple compositions and configurations for dual-doped graphene-based electrocatalysts have been produced.

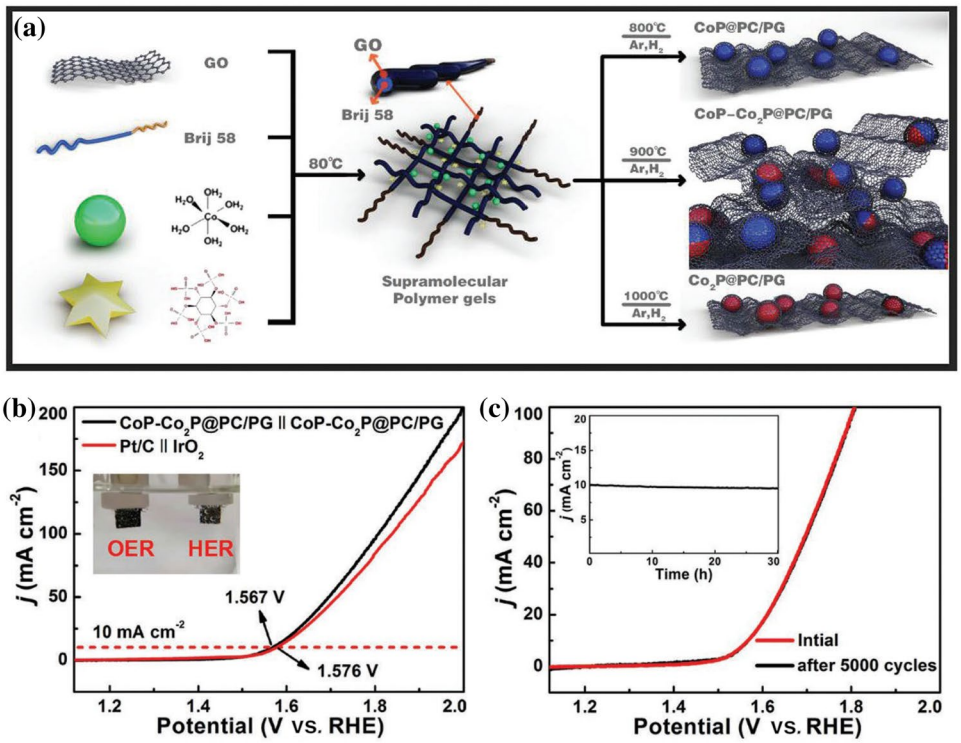

Fig. 14 **a** Schematic of the synthesis of CoP–Co_2P@P–C/P–GN, Co_2P@P–C/P–GN and CoP@P–C/P–GN electrocatalysts. **b** LSV curves of CoP-Co_2P@PC/P-GN‖CoP–Co_2P@PC/P–GN and Pt/C‖IrO_2 for OWS in 1.0 M KOH solution. Inset exhibits the water electrolyzer for OWS. **c** Stability test of CoP-Co_2P@PC/P-GN‖CoP-Co_2P@PC/P-GN for OWS. Inset shows the chronoamperometry curve at 1.567 V (vs RHE). Reprinted with permission [136]. Copyright 2019 John Wiley and Sons

4.4.2.1 Nitrogen and Sulfur Co-doped Graphene N, S co-doped graphene-based electrocatalysts are favorable and green replacements for precious metal electrocatalysts for OWS reactions [140]. Based on this, Xu et al. [38] developed a novel turnover frequency (TOF) calculation strategy to identify the active site reactivity of electrocatalysts as well as both structural and heteroatoms defects and found that activated graphene can provide better electrocatalytic performances than graphene for HER and OER, suggesting that structural defects can allow for substantial improvements. And based on their DFT calculations as well as the electrocatalytic activities of various graphene-based electrocatalysts, these researchers suggested that doped elements should be kept together if the descriptors of one co-doped element were much smaller than N and that co-doped elements with relatively different chemical properties should be selected to achieve better results. Liu et al. [141] also developed an in situ method to synthesize ultrathin Co_9S_8 nanosheets vertically loaded on N, S co-doped reduced graphene oxide (NS-rGO) as an efficient and novel electrocatalyst for OWS and reported that the obtained morphology with vertically loaded Co_9S_8 nanosheets on NS-rGO can promote the transportation of electrons and exposure of active sites. And based on the synergetic electrocatalysis between NS-rGO and Co_9S_8, these researchers reported that their Co_9S_8/NS-rGO electrocatalyst exhibited excellent performances toward OER and HER with low overpotentials of 266 and 332.4 mV, respectively, to obtain a

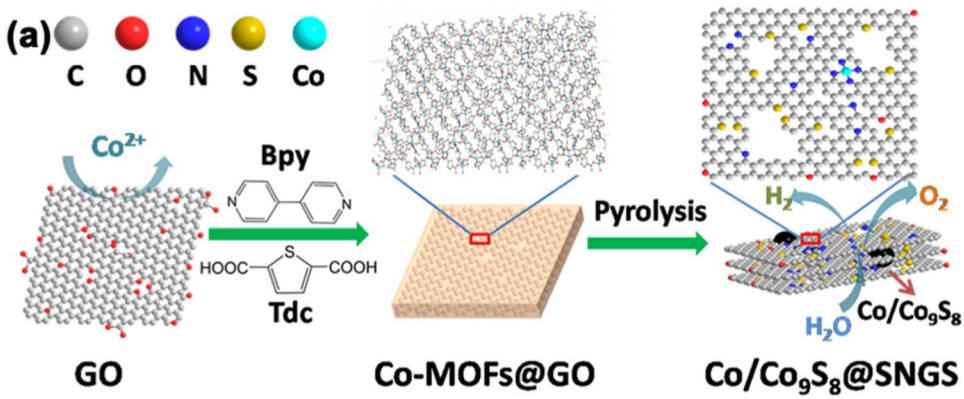

Fig. 15 Schematic of the synthesis of a Co/Co_9S_8@SN-GS electrocatalyst derived from Co-MOFs@GO. Reprinted with permission [142]. Copyright 2019 Elsevier

electrocatalysts in a broad range of applications.

current density of 10 mA cm^{-2} in alkaline media. Similarly, Zhang et al. [142] synthesized Co/Co_9S_8 core–shell nanostructures loaded on N, S co-doped porous-shaped graphene nanosheets (Co/Co_9S_8@SN-GN) as an electrocatalyst by using Co-based metal organic frameworks (Co-MOFs) on graphene oxide nanosheets (Co-MOFs@GO) in the presence of 4,4´-bipyridine (Bpy) and thiophene-2, 5-dicarboxylate (Tdc) dual organic ligands in a NaOH/H_2O system at room temperature (Fig. 15) and reported that the bifunctional Co/Co_9S_8@SN-GN hybrid can provide excellent electrocatalytic activities toward both HER and OER in 0.1 M KOH.

Overall, N and S are significant dopants for graphene nanomaterials in OWS applications and can open new avenues of development for graphene-based electrocatalysts in a broad range of applications.

4.4.2.2 Nitrogen and Fluorine Co-doped Graphene N, F co-doped porous graphene nanosheets (NFPGNS) can also act as metal-free bifunctional electrocatalysts for OWS. Based on this, Yue et al. [35] obtained chronoamperometric plots for HER and OER using a NFPGNS nanohybrid at a cell voltage of 1.57 and − 0.33 V versus RHE (Fig. 16a) and reported that the onset voltage of OWS with NFPGNS was lower than the potential of 1.60 V, which is slightly higher than that of commercial Pt/C electrocatalysts (Fig. 16b). In addition, chronoamperometric plots revealed that for the NFPGNS electrocatalyst for OWS at 1.91 V, the initial current density of 10.0 mA cm^{-2} gradually declined to a current density of 8.2 mA cm^{-2} after 12 h (Fig. 16c). Here, these researchers suggested that the Co-doped graphene-modified electron acceptor–donor quality of the carbon as induced by the synergistic interactions between heteroatoms can introduce promising electronic nanostructures to tune C sites that are surrounded by heteroatoms.

4.4.2.3 Nitrogen and Phosphorous Co-doped Graphene In terms of N, P co-doped graphene, researchers have reported that N, P co-doped defects can provide better performances than single N- and P-doped defects because N dopants can decrease the displacement created by P dopants to create a damping effect on structural distortions [143]. Based on this, Liu et al. [116] designed an active, stable and earth-abundant OWS electrocatalyst that works in the same solution involving CoP nanoparticles loaded on N, P co-doped mesoporous graphene (CoP/NP-MG). And as a result, the obtained CoP/NP-MG electrocatalyst exhibited remarkable bifunctional performances over a wide pH range in which excellent activities at cell voltages of 1.58 V (1 M KOH) and 1.74 V (1.0 M phosphate-buffered saline) with a current density of 10 mA cm^{-2} can be obtained as well as remarkable electrocatalytic stability at all pH ranges. In another example, Das et al. [144] developed a facile one-step approach to prepare a hybrid of Co_2P anchored on N, P co-doped graphene nanotubes (Co_2P/NP-GNTs) in which SEM and TEM images (Fig. 17a,b) confirmed that Co_2P nanoparticles were almost encapsulated within thin walls of N, P co-doped graphene nanotubes. Here, these researchers

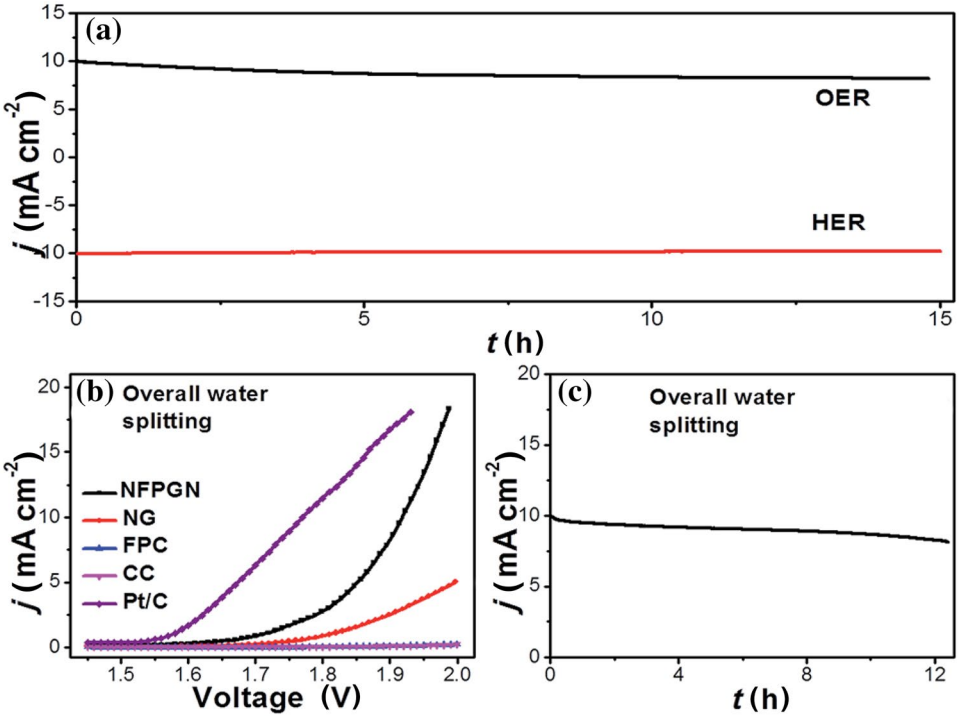

Fig. 16 **a** Chronoamperometric study for OER at 1.57 V and HER at − 0.33 V versus RHE used a NFPGNS hybrid in 1.0 M KOH at room temperature. **b** LSV curves of NFPGNS, N-GN, FPC, CC and commercial Pt/C electrocatalysts for OWS in 1.0 M KOH at room temperature. **c** Chronoamperometry study of OWS at a cell voltage of 1.91 V on a NFPGNS electrocatalyst in 1.0 M KOH solution at room temperature. Reprinted with permission [35]. Copyright 2017 Royal Society of Chemistry

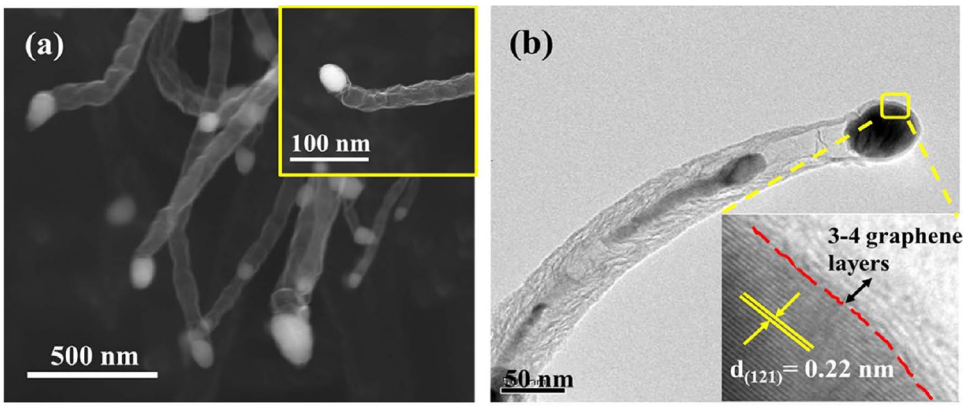

Fig. 17 **a** SEM (inset: isolated nanotube) and **b** TEM images (inset: HRTEM image) of a Co_2P/NP-GNTs hybrid. Reprinted with permission [144]. Copyright 2019 Elsevier

reported that the hybrid possessed a lattice fringe of 2.2 nm that corresponded to the (121) plane of Co_2P nanoparticles anchored within 3–4 layers of N, P co-doped graphene with an 0.346 nm interlayer space, resulting in Van der Waals attraction, which can enhance the stability of the electrocatalyst. And as a result, the Co_2P/NP-GNTs hybrid demonstrated remarkable bifunctional HER and OER electrocatalytic performances with a current density of a 10 mA cm^{-2} at 1.53 V.

4.4.2.4 Nitrogen and Oxygen Co-doped Graphene To date, N, O co-doped bifunctional electrocatalysts for OWS have rarely been reported. However, Hu et al. [145] developed a feasible strategy to synthesize N, O co-doped graphene nanoring-integrated boxes (NO-GB) through the high-temperature pyrolysis and successive acid etching of nanohybrid precursors including polydopamine (PDA) coated with CoCo-Prussian blue analogue (CoCo-PBA) cubes (Fig. 18) and reported that the obtained hollow graphene nanorings possessed a hierarchical mesoporous nanostructure that can provide large numbers of accessible active sites and promote the mass transport kinetics of electrocatalysis. In addition, these researchers suggested that the introduction of O to N-doped graphene can enhance the formation of C^+ active sites to allow for significant increases to HER and OER performance. And as a result, the bifunctional NO-GB hybrid demonstrated remarkable activity for OWS to obtain a current density of 10 mA cm^{-2} at 1.65 V.

4.4.2.5 Nitrogen and Boron Co-doped Graphene As for N, B co-doping, the abundance of C–N and C–B nanostructures at different compositional ranges in corresponding catalysts can allow for promising electronic structures to provide more accessible active sites for OWS and enhance performance [146, 147]. Based on this, Zhang et al. [148] used N, B co-doped graphene (NB-GN) as an electroactive support material for $CoMoS_{3.13}$ nanoparticles to synthesize a bifunctional electrocatalyst for OWS in which N and B atoms can serve as electroactive sites to promote OWS and NB-GN supported materials can provide terminated textured edges of $CoMoS_{3.13}$ to generate more active sites and act as a medium to boost charge transport for rapid reaction kinetics.

4.4.2.6 Nitrogen and Cobalt Co-doped Graphene Zhou et al. [149] also used an extended dual-doping strategy to obtain an N, Co co-doped graphene with low-coordinated Co sites to allow for enhanced electrocatalytic HER performances with a calculated adsorption free energy of −0.01 eV for hydrogen and a high-coordinated Co center to allow for enhanced electrocatalytic OER performances with a low overpotential of −0.39 V, thus demonstrating the

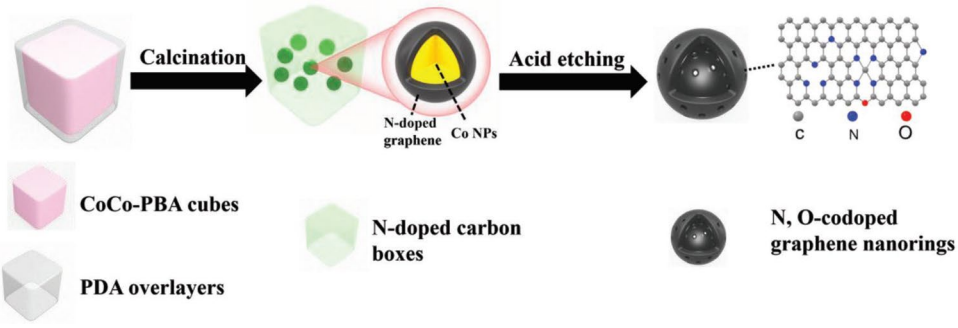

Fig. 18 Schematic for the synthesis of N, O co-doped graphene nanoring-integrated boxes (NO-GB) through the high-temperature pyrolysis and successive acid etching of nanohybrid precursors including polydopamine (PDA)-coated CoCo-Prussian blue analogue (CoCo-PBA) cubes. Reprinted with permission [145]. Copyright 2019 John Wiley and Sons

potential of N, Co co-doped graphene as a bifunctional electrocatalyst for OWS.

4.4.3 Tri-Doped Graphene

And of particular interest, the co-doping of graphene with three hetero-elements of different electronegativities than carbon atoms have been reported to also be able to better promote OWS based on synergetic interactions as compared with single- and dual-doped counterparts in which tri-doped graphene nanomaterials can possess bifunctional active sites for HER and OER simultaneously. For example, Zhang et al. [150] synthesized N, P and F tri-doped graphene through thermal activation (Fig. 19a) using a mixture of ammonium hexafluorophosphate and polyaniline-coated graphene oxide for OWS and reported that this integrated metal-free electrocatalyst possessed self-powered OWS abilities and can generate H_2 and O_2 at large rates of 0.496 and 0.254 μL s^{-1}, respectively, thus showing promise for industrial application. In another study, Zhang et al. [107] loaded Co nanoparticles on N, S and Co tri-doped graphene at 900 °C (SSUCo-900) and reported that this tri-doped SSUCo-900 catalyst can maintain a current density of 10 and 100 mA cm^{-2} at cell voltages 1.88 and 2.20 V, respectively, and provide vigorous electron transfer reactions on both the anode and cathode based on the distinctive bubbles of O_2 and H_2 liberated at electrodes (Fig. 19b, c). In addition, these researchers reported that the Faradaic efficiency for both OER and HER as close to 100% (Fig. 19d), suggesting remarkable performances for OWS. Here, these researchers used a water splitting electrolyzer consisting of the SSUCo-900 electrocatalyst to study long-term stability and reported that the SSUCo-900 electrocatalyst maintained a current density of 50 mA cm^{-2} for 7 h and that after testing, the polarization curve was almost identical to the initial curve, thus exhibiting superior durability for OWS (Fig. 19e).

Overall, the electrocatalytic activity of electrocatalysts is mainly based on the synergistic effects arising from nanoparticle cores and heteroatom-doped graphene. Therefore, various approaches including the optimization of compositions, the further enhancement of surface areas and the reduction in the thickness of graphene nanosheet-enclosed nanoparticles are all viable methods to further boost the bifunctional activity of tri-doped graphene.

5 Conclusions and Future Perspective

Overall, the development of electroactive, earth-abundant and robust OWS electrocatalysts for the production of H_2 and O_2 is a critical challenge in the development of eco-friendly, economical and efficient renewable energy interconversion technologies. To address this, this review has presented the latest progress in graphene-based OWS

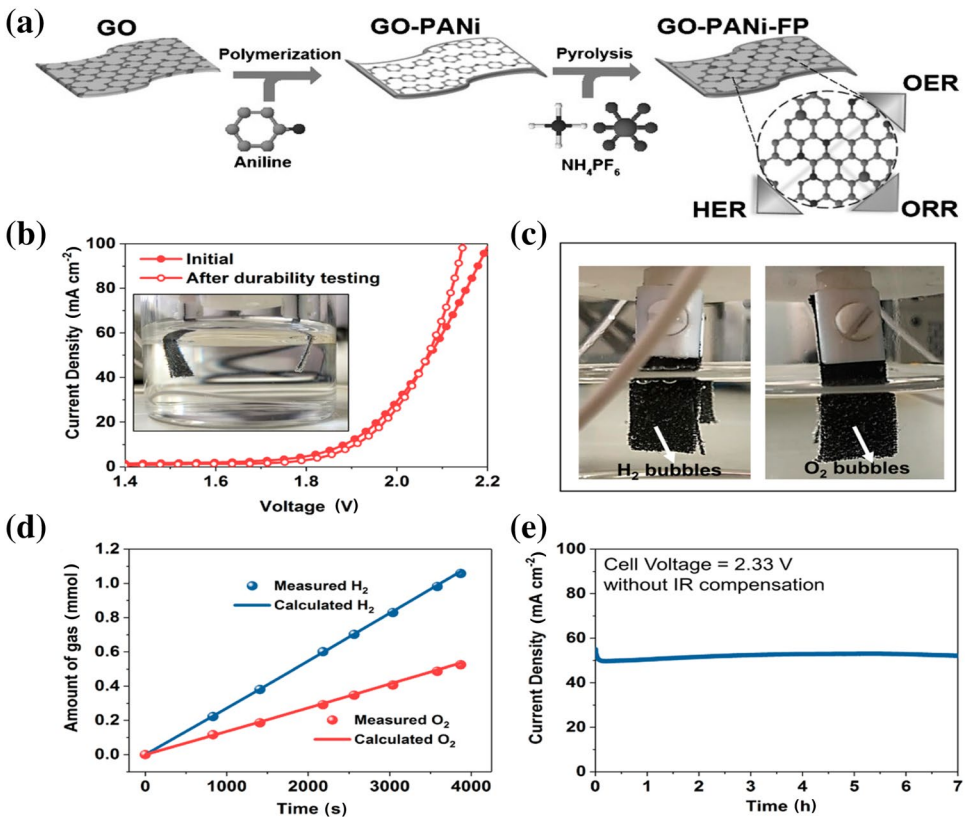

Fig. 19 **a** Schematic of a N, P and F tri-doped graphene electrocatalyst for OWS. Reprinted with permission [150]. Copyright 2016 John Wiley and Sons. **b** Initial and final polarization curves obtained using the SUCo-900 electrocatalyst for OWS in 1.0 M KOH at 5 mV s^{-1}. **c** Image showing the evolution of O_2 and H_2 bubbles. **d** Experimental versus theoretical amounts of generated O_2 and H_2 for the SSUCo-900 electrocatalyst for OWS. **e** Time-dependent study of current density at 2.33 V for a water electrolyzer using the SSUCo-900 electrocatalyst. Reprinted with permission [107]. Copyright 2017 American Chemical Society

electrocatalysts, including corresponding electrochemistry, topological effects, edge engineering, interface effects, support effects as well as applications. And with great efforts from researchers in the last decade to developed novel graphene-based electrocatalysts to decrease or substitute precious metal-based electrocatalysts accompanied by major breakthroughs in nanotechnology and materials science, graphene-based electrocatalysts have gained substantial prominence for OWS applications. Here, synergistic effects between graphene and nanoparticles as well as other conductive materials can lead to increased electrical conductivity and surface area to lower OWS reaction overpotentials. In addition, advancements in graphene-based bifunctional electrocatalysts can enable the design of optimal water splitting electrolyzer systems and address related issues surrounding corresponding electrocatalysts. Furthermore, graphene and activated graphene can be used as supporting materials for many non-precious nanoparticles such as Ni or Co and various functional heteroatom-doped graphene materials can present distinctive features that can significantly enhance OWS due to their numerous active sites, controllable morphology and high tolerance to acidic/alkaline media.

Despite these advancements however, OWS efficiency for H_2 and O_2 generation remains comparatively low for many graphene-based electrocatalysts and supplemental electrocatalysts are generally required to resolve complications that can impede performance. In addition, several challenges remain, and future research needs to focus on several directions to further enhance graphene-based electrocatalysts for OWS:

1. The electrocatalytic activity of graphene-based electrocatalysts needs to be further optimized. Although the design of multi-dimensional graphene materials that possess unique features as compared with pristine graphene sheets has been reported, challenges remain. For example, the precise control of the size and width of carbon materials is necessary during synthesis because current-carrying capacity and spin-polarized edge states greatly depend on crystallographic orientation, width and edge structure. In addition, graphene-based nanomaterials tend to reaggregate or restack in the course of their practical use due to Van der Waals forces between adjacent carbon nanosheets, which can lead to the disappearance of the unique structural merits associated with separated graphene nanosheets and the coverage of considerable portions of electrochemically active sites, all of which can result in large losses to catalytic activity. Based on this, a deeper understanding of these graphene materials is required for the effective design and construction of superior structures.
2. A deeper understanding of the catalysis mechanisms of OWS at the molecular level based on theoretical and experimental investigations is required and can enable the design of effective bifunctional electrocatalysts. In addition, the gap between theoretical computations and experimental results for graphene-based electrocatalysts needs to be filled and will require close collaboration between electrochemists and computational scientists. Furthermore, unlike metallic electrocatalysts, a deeper comprehension of the specific effects of geometrical and electronic states toward reaction intermediates in graphene-based electrocatalysts is also required.
3. A basic understanding of electrocatalytically active sites on graphene-based electrocatalysts is needed, especially for doped graphene. Here, researchers need to pay more attention to the development of more active and durable OWS electrocatalysts and apply different characterization and analytical techniques to confirm actual catalytic active sites to study electrochemical reaction processes.
4. Currently, most research is focused on bifunctional electrocatalysts in alkaline media, which excludes possible operation in water electrolyzers based on proton exchange membranes. Therefore, acid-stable graphene-based electrocatalysts with excellent performance and stability are required, especially for anodic OER.
5. More attention needs to be paid to tri-doped graphene-based electrocatalysts for OWS, especially the development of multi-doped graphene-based nanomaterials. And as electrocatalysts involving multi-doped graphene become more complex, actual active sites become more difficult to differentiate, meaning that a fundamental comprehension of the OWS mechanisms of multi-doped graphene-based electrocatalysts is required aside from current calculation and modeling techniques.
6. Because morphology and composition are vital factors responsible for the performance and stability of electrocatalysts, ideal electrocatalysts with remarkable stability can only be obtained if stability factors are well-controlled and fully identified. However, increases in electrocatalytic performance usually correspond to decreases in catalyst stability for OWS. Therefore, more advanced synthesis strategies are required to prepare graphene-based nanomaterials with higher chemical and mechanical stability to withstand unfavorable environments during OWS. In addition, the control and identification of stability parameters such as the catalyst phase/composition, substrate materials, electrode–electrolyte wettability, the catalyst/substrate interface, mechanical characteristics are also required to synthesize robust graphene-supported electrocatalysts. Furthermore, because the undesirable correlation between performance and stability is not yet fully understood for many electrocatalysts, more research is required to achieve balanced activities.

7. Despite OER performances of some graphene-based electrocatalysts being almost comparable to noble metal-based electrocatalysts, HER performances remain seriously lacking as compared with metal-based counterparts based on experimental evidence and DFT calculations. Therefore, further research on basic principles is required to gain full comprehension of the origin for performance enhancement.

Overall, rational efforts and close cooperation from a wide range of scientific fields can lead to future breakthroughs in the development of OWS technologies.

Acknowledgements This work was supported by the Guangxi Science and Technology Project (AA17204083, AB16380030), the link project of the National Natural Science Foundation of China and Fujian Province (U1705252) and the Natural Science Foundation of Guangdong Province (2015A030312007).

References

1. Jamesh, M.I., Kuang, Y., Sun, X.: Constructing earth-abundant 3D nanoarrays for efficient overall water splitting–a review. J. ChemCatChem **11**, 1550–1575 (2019)
2. Tam, T.V., Kang, S.G., Kim, M.H., et al.: Novel graphene hydrogel/b-doped graphene quantum dots composites as trifunctional electrocatalysts for Zn–Air batteries and overall water splitting. Adv. Energy Mater. **9**, 1900945 (2019)
3. Yu, L., Zhou, H., Sun, J., et al.: Cu nanowires shelled with NiFe layered double hydroxide nanosheets as bifunctional electrocatalysts for overall water splitting. Energy Environ. Sci. **10**, 1820–1827 (2017)
4. Xue, Q., Ding, Y., Xue, Y., et al.: 3D nitrogen-doped graphene aerogels as efficient electrocatalyst for the oxygen reduction reaction. Carbon **139**, 137–144 (2018)
5. Zhou, W., Jia, J., Lu, J., et al.: Recent developments of carbon-based electrocatalysts for hydrogen evolution reaction. Nano Energy **28**, 29–43 (2016)
6. Chen, Z., Ha, Y., Jia, H., et al.: Oriented transformation of Co-LDH into 2D/3D ZIF-67 to achieve Co–N–C hybrids for efficient overall water splitting. Adv. Energy Mater. **9**, 1803918 (2019)
7. Lv, Y., Wang, X.: Nonprecious metal phosphides as catalysts for hydrogen evolution, oxygen reduction and evolution reactions. Catal. Sci. Technol. **7**, 3676–3691 (2017)
8. Sun, H., Yan, Z., Liu, F., et al.: Self-supported transition-metal-based electrocatalysts for hydrogen and oxygen evolution. Adv. Mater. **32**, 1806326 (2019)
9. Kuang, P., He, M., Zou, H., et al.: 0D/3D MoS_2-NiS_2/N-doped graphene foam composite for efficient overall water splitting. Appl. Catal. B **254**, 15–25 (2019)
10. Liang, H., Gandi, A.N., Anjum, D.H., et al.: Plasma-assisted synthesis of NiCoP for efficient overall water splitting. Nano Lett. **16**, 7718–7725 (2016)
11. Ling, C., Shi, L., Ouyang, Y., et al.: Nanosheet supported single-metal atom bifunctional catalyst for overall water splitting. Nano Lett. **17**, 5133–5139 (2017)
12. Wang, J., Zhong, H.-X., Wang, Z.-L., et al.: Integrated three-dimensional carbon paper/carbon tubes/cobalt-sulfide sheets as an efficient electrode for overall water splitting. ACS Nano **10**, 2342–2348 (2016)
13. Zhang, J., Zhang, Q., Feng, X.: Support and interface effects in water-splitting electrocatalysts. Adv. Mater. **31**, 1808167 (2019)
14. Li, M., Zhu, Y., Wang, H., et al.: Ni strongly coupled with Mo2C encapsulated in nitrogen-doped carbon nanofibers as robust bifunctional catalyst for overall water splitting. Adv. Energy Mater. **9**, 1803185 (2019)
15. Zhang, X., Xu, H., Li, X., et al.: Facile synthesis of nickel–iron/nanocarbon hybrids as advanced electrocatalysts for efficient water splitting. ACS Catal. **6**, 580–588 (2016)
16. Zhu, J., Sakaushi, K., Clavel, G., et al.: A general salt-templating method to fabricate vertically aligned graphitic carbon nanosheets and their metal carbide hybrids for superior lithium ion batteries and water splitting. J. Am. Chem. Soc. **137**, 5480–5485 (2015)
17. Lu, C., Tranca, D., Zhang, J., et al.: Molybdenum carbide-embedded nitrogen-doped porous carbon nanosheets as electrocatalysts for water splitting in alkaline media. ACS Nano **11**, 3933–3942 (2017)
18. Masa, J., Weide, P., Peeters, D., et al.: Amorphous cobalt boride (Co2B) as a highly efficient nonprecious catalyst for electrochemical water splitting: oxygen and hydrogen evolution. Adv. Energy Mater. **6**, 1502313 (2016)
19. Fominykh, K., Chernev, P., Zaharieva, I., et al.: Iron-doped nickel oxide nanocrystals as highly efficient electrocatalysts for alkaline water splitting. ACS Nano **9**, 5180–5188 (2015)
20. Shalom, M., Ressnig, D., Yang, X., et al.: Nickel nitride as an efficient electrocatalyst for water splitting. J. Mater. Chem. A **3**, 8171–8177 (2015)
21. Pan, Z., Zheng, Y., Guo, F., et al.: Decorating CoP and Pt nanoparticles on graphitic carbon nitride nanosheets to promote overall water splitting by conjugated polymers. Chemsuschem **10**, 87–90 (2017)
22. Du, L., Shao, Y., Sun, J., et al.: Advanced catalyst supports for PEM fuel cell cathodes. Nano Energy **29**, 314–322 (2016)
23. Rostami, H., Rostami, A.A., Omrani, A.: Investigation on ethanol electrooxidation via electrodeposited Pd–Co nanostructures supported on graphene oxide. Int. J. Hydrog. Energy **40**, 10596–10604 (2015)
24. Duan, J., Chen, S., Vasileff, A., et al.: Anion and cation modulation in metal compounds for bifunctional overall water splitting. ACS Nano **10**, 8738–8745 (2016)
25. Hou, J., Sun, Y., Cao, S., et al.: Graphene dots embedded phosphide nanosheet-assembled tubular arrays for efficient and stable overall water splitting. ACS Appl. Mater. **9**, 24600–24607 (2017)
26. Govindhan, M., Mao, B., Chen, A.: Novel cobalt quantum dot/graphene nanocomposites as highly efficient electrocatalysts for water splitting. Nanoscale **8**, 1485–1492 (2016)
27. Molina-García, M.A., Rees, N.V.: "Metal-free" electrocatalysis: quaternary-doped graphene and the alkaline oxygen reduction reaction. Appl. Catal. A **553**, 107–116 (2018)
28. Novoselov, K.S., Geim, A.K., Morozov, S.V., et al.: Electric field effect in atomically thin carbon films. Science **306**, 666–669 (2004)
29. Liu, J., Ma, Q., Huang, Z., et al.: Recent progress in graphene-based noble-metal nanocomposites for electrocatalytic applications. Adv. Mater. **31**, 1800696 (2019)
30. Wang, C., Astruc, D.: Recent developments of metallic nanoparticle-graphene nanocatalysts. Prog. Mater Sci. **94**, 306–383 (2018)
31. Liu, H.L., Nosheen, F., Wang, X.: Noble metal alloy complex nanostructures: controllable synthesis and their electrochemical property. Chem. Soc. Rev. **44**, 3056–3078 (2015)

32. Duan, J., Chen, S., Jaroniec, M., et al.: Heteroatom-doped graphene-based materials for energy-relevant electrocatalytic processes. ACS Catal. **5**, 5207–5234 (2015)
33. Ito, Y., Cong, W., Fujita, T., et al.: High catalytic activity of nitrogen and sulfur co-doped nanoporous graphene in the hydrogen evolution reaction. Angew. Chem. Int. Ed. **54**, 2131–2136 (2015)
34. Yu, X., Zhang, S., Li, C., et al.: Hollow CoP nanopaticle/N-doped graphene hybrids as highly active and stable bifunctional catalysts for full water splitting. Nanoscale **8**, 10902–10907 (2016)
35. Yue, X., Huang, S., Cai, J., et al.: Heteroatoms dual doped porous graphene nanosheets as efficient bifunctional metal-free electrocatalysts for overall water-splitting. J. Mater. Chem. A **5**, 7784–7790 (2017)
36. Xu, X., Liang, H., Tang, G., et al.: Accelerating the water splitting kinetics of CoP microcubes anchored on a graphene electrocatalyst by Mn incorporation. Nanoscale Adv. **1**, 177–183 (2019)
37. Jamesh, M.I.: Recent progress on earth abundant hydrogen evolution reaction and oxygen evolution reaction bifunctional electrocatalyst for overall water splitting in alkaline media. J. Power Sources **333**, 213–236 (2016)
38. Xu, Y., Kraft, M., Xu, R.: Metal-free carbonaceous electrocatalysts and photocatalysts for water splitting. Chem. Soc. Rev. **45**, 3039–3052 (2016)
39. Yan, Y., Xia, B.Y., Zhao, B., et al.: A review on noble-metal-free bifunctional heterogeneous catalysts for overall electrochemical water splitting. J. Mater. Chem. A **4**, 17587–17603 (2016)
40. Han, N., Liu, P., Jiang, J., et al.: Recent advances in nanostructured metal nitrides for water splitting. J. Mater. Chem. A **6**, 19912–19933 (2018)
41. Shi, Q., Zhu, C., Du, D., et al.: Robust noble metal-based electrocatalysts for oxygen evolution reaction. Chem. Soc. Rev. **48**, 3181–3192 (2019)
42. Shi, Y., Yu, Y., Liang, Y., et al.: In situ electrochemical conversion of an ultrathin tannin nickel iron complex film as an efficient oxygen evolution reaction electrocatalyst. Angew. Chem. Int. Ed. **58**, 3769–3773 (2019)
43. Zhang, Z., Zhou, D., Wu, X., et al.: Synthesis of La0.2Sr0.8CoO3 and its electrocatalytic activity for oxygen evolution reaction in alkaline solution. Int. J. Hydrog. Energy **44**, 7222–7227 (2019)
44. Zhou, W., Huang, D.D., Wu, Y.P., et al.: Stable hierarchical bimetal-organic nanostructures as highperformance electrocatalysts for the oxygen evolution reaction. Angew. Chem. Int. Ed. **58**, 4227–4231 (2019)
45. Dong, X., Yan, H., Jiao, Y., et al.: 3D hierarchical V-Ni-based nitride heterostructure as a highly efficient pH-universal electrocatalyst for the hydrogen evolution reaction. J. Mater. Chem. A **7**, 15823–15830 (2019)
46. Pu, Z., Zhao, J., Amiinu, I.S., et al.: A universal synthesis strategy for P-rich noble metal diphosphide-based electrocatalysts for the hydrogen evolution reaction. Energy Environ. Sci. **12**, 952–957 (2019)
47. Jin, H., Liu, X., Chen, S., et al.: Heteroatom-doped transition metal electrocatalysts for hydrogen evolution reaction. ACS Energy Lett. **4**, 805–810 (2019)
48. Liu, T., Li, P., Yao, N., et al.: CoP-doped MOF-based electrocatalyst for pH-universal hydrogen evolution reaction. Angew. Chem. Int. Ed. **58**, 4679–4684 (2019)
49. You, B., Sun, Y.: Innovative strategies for electrocatalytic water splitting. Acc. Chem. Res. **51**, 1571–1580 (2018)
50. Ullah, N., Zhao, W., Lu, X., et al.: In situ growth of M-MO (M = Ni, Co) in 3D graphene as a competent bifunctional electrocatalyst for OER and HER. Electrochim. Acta **298**, 163–171 (2019)
51. Xiu, L., Wang, Z., Yu, M., et al.: Aggregation-resistant 3D MXene-based architecture as efficient bifunctional electrocatalyst for overall water splitting. ACS Nano **12**, 8017–8028 (2018)
52. Xiong, B., Chen, L., Shi, J.: Anion-containing noble-metal-free bifunctional electrocatalysts for overall water splitting. ACS Catal. **8**, 3688–3707 (2018)
53. Zou, X., Zhang, Y.: Noble metal-free hydrogen evolution catalysts for water splitting. Chem. Soc. Rev. **44**, 5148–5180 (2015)
54. Wang, J., Xu, F., Jin, H., et al.: Non-noble metal-based carbon composites in hydrogen evolution reaction: fundamentals to applications. Adv. Mater. **29**, 1605838 (2017)
55. Jiao, L., Zhou, Y.-X., Jiang, H.-L.: Metal–organic framework-based CoP/reduced graphene oxide: high-performance bifunctional electrocatalyst for overall water splitting. Chem. Sci. **7**, 1690–1695 (2016)
56. Li, X., Duan, X., Han, C., et al.: Chemical activation of nitrogen and sulfur co-doped graphene as defect-rich carbocatalyst for electrochemical water splitting. Carbon **148**, 540–549 (2019)
57. Boukhvalov, D.W., Son, Y.-W., Ruoff, R.S.: Water splitting over graphene-based catalysts: ab initio calculations. ACS Catal. **4**, 2016–2021 (2014)
58. Gu, Y., Chen, S., Ren, J., et al.: Electronic structure tuning in Ni_3FeN/r-GO aerogel toward bifunctional electrocatalyst for overall water splitting. ACS Nano **12**, 245–253 (2018)
59. Tsai, H.-C., Vedhanarayanan, B., Lin, T.-W.: Freestanding and hierarchically structured Au-dendrites/3D-graphene scaffold supports highly active and stable Ni3S2 electrocatalyst towards overall water splitting. ACS Appl. Energy Mater. **2**, 3708–3716 (2019)
60. Huang, H., Ma, L., Tiwary, C.S., et al.: Worm-shape Pt nanocrystals grown on nitrogen-doped low-defect graphene sheets: highly efficient electrocatalysts for methanol oxidation reaction. Small **13**, 1603013 (2017)
61. Tang, C., Wang, B., Wang, H.-F., et al.: Defect engineering toward atomic Co–N_x–C in hierarchical graphene for rechargeable flexible solid Zn-air batteries. Adv. Mater. **29**, 1703185 (2017)
62. Park, M., Jeon, I.-Y., Ryu, J., et al.: Exploration of the effective location of surface oxygen defects in graphene-based electrocatalysts for all-vanadium redox-flow batteries. Adv. Energy Mater. **5**, 1401550 (2015)
63. Wang, Q., Ji, Y., Lei, Y., et al.: Pyridinic-N-dominated doped defective graphene as a superior oxygen electrocatalyst for ultrahigh-energy-density Zn–air batteries. ACS Energy Lett. **3**, 1183–1191 (2018)
64. Wu, J., Liu, M., Sharma, P.P., et al.: Incorporation of nitrogen defects for efficient reduction of CO_2 via two-electron pathway on three-dimensional graphene foam. Nano Lett. **16**, 466–470 (2016)
65. Wang, X., Vasileff, A., Jiao, Y., et al.: Electronic and structural engineering of carbon-based metal-free electrocatalysts for water splitting. Adv. Mater. **31**, 1803625 (2019)
66. Tao, L., Wang, Q., Dou, S., et al.: Edge-rich and dopant-free graphene as a highly efficient metal-free electrocatalyst for the oxygen reduction reaction. Chem. Commun. **52**, 2764–2767 (2016)
67. Liu, Z., Zhao, Z., Wang, Y., et al.: In situ exfoliated, edge-rich, oxygen-functionalized graphene from carbon fibers for oxygen electrocatalysis. Adv. Mater. **29**, 1606207 (2017)
68. Park, M., Jeon, I.-Y., Ryu, J., et al.: Edge-halogenated graphene nanoplatelets with F, Cl, or Br as electrocatalysts for all-vanadium redox flow batteries. Nano Energy **26**, 233–240 (2016)
69. Wang, H., Li, X.-B., Gao, L., et al.: Three-dimensional graphene networks with abundant sharp edge sites for efficient electrocatalytic hydrogen evolution. Angew. Chem. **130**, 198–203 (2018)

70. Xiao, Z., Huang, X., Xu, L., et al.: Edge-selectively phosphorus-doped few-layer graphene as an efficient metal-free electrocatalyst for the oxygen evolution reaction. Chem. Commun. **52**, 13008–13011 (2016)
71. Matanovic, I., Artyushkova, K., Strand, M.B., et al.: Core level shifts of hydrogenated pyridinic and pyrrolic nitrogen in the nitrogen-containing graphene-based electrocatalysts: in-plane vs edge defects. J. Phys. Chem. C **120**, 29225–29232 (2016)
72. Zhang, L., Jia, Y., Gao, G., et al.: Graphene defects trap atomic Ni species for hydrogen and oxygen evolution reactions. Chem **4**, 285–297 (2018)
73. Chen, Z., Xu, H., Ha, Y., et al.: Two-dimensional dual carbon-coupled defective nickel quantum dots towards highly efficient overall water splitting. Appl. Catal. B Environ. **250**, 213–223 (2019)
74. Lu, Y., Hou, W., Yang, D., et al.: CoP nanosheets in situ grown on N-doped graphene as an efficient and stable bifunctional electrocatalyst for hydrogen and oxygen evolution reactions. Electrochim. Acta **307**, 543–552 (2019)
75. Yang, J., Xing, S., Zhou, J., et al.: The controlled construction of a ternary hybrid of monodisperse Ni3S4 nanorods/graphitic C3N4 nanosheets/nitrogen-doped graphene in van der Waals heterojunctions as a highly efficient electrocatalyst for overall water splitting and a promising anode material for sodium-ion batteries. J. Mater. Chem. A **7**, 3714–3728 (2019)
76. Yang, Y., Lin, Z., Gao, S., et al.: Tuning electronic structures of nonprecious ternary alloys encapsulated in graphene layers for optimizing overall water splitting activity. ACS Catal. **7**, 469–479 (2016)
77. Li, X., Zhang, L., Huang, M., et al.: Cobalt and nickel selenide nanowalls anchored on graphene as bifunctional electrocatalysts for overall water splitting. J. Mater. Chem. A **4**, 14789–14795 (2016)
78. Jia, Y., Zhang, L., Du, A., et al.: Defect graphene as a trifunctional catalyst for electrochemical reactions. Adv. Mater. **28**, 9532–9538 (2016)
79. Xu, Y., Tu, W., Zhang, B., et al.: Nickel nanoparticles encapsulated in few-layer nitrogen-doped graphene derived from metal-organic frameworks as efficient bifunctional electrocatalysts for overall water splitting. Adv. Mater. **29**, 1605957 (2017)
80. Li, J., Zhang, X., Zhang, Z., et al.: Graphene-quantum-dots-induced facile growth of porous molybdenum doped Ni_3S_2 nanoflakes as efficient bifunctional electrocatalyst for overall water splitting. Electrochim. Acta **304**, 487–494 (2019)
81. Zhao, M., Zhang, J., Xiao, H., et al.: Facile in situ synthesis of a carbon quantum dot/graphene heterostructure as an efficient metal-free electrocatalyst for overall water splitting. Chem. Commun. **55**, 1635–1638 (2019)
82. Jia, Y., Zhang, L., Gao, G., et al.: A heterostructure coupling of exfoliated Ni–Fe hydroxide nanosheet and defective graphene as a bifunctional electrocatalyst for overall water splitting. Adv. Mater. **29**, 1700017 (2017)
83. Wu, J., Ren, Z., Du, S., et al.: A highly active oxygen evolution electrocatalyst: ultrathin CoNi double hydroxide/CoO nanosheets synthesized via interface-directed assembly. Nano Res. **9**, 713–725 (2016)
84. Li, Y., Yin, J., An, L., et al.: FeS_2/CoS_2 interface nanosheets as efficient bifunctional electrocatalyst for overall water splitting. Small **14**, 1801070 (2018)
85. Velasco-Velez, J.J., Pfeifer, V., Hävecker, M., et al.: Photoelectron spectroscopy at the graphene-liquid interface reveals the electronic structure of an electrodeposited cobalt/graphene electrocatalyst. Angew. Chem. Int. Ed. **54**, 14554–14558 (2015)
86. Zhang, J., Wang, T., Pohl, D., et al.: Interface engineering of MoS_2/Ni_3S_2 heterostructures for highly enhanced electrochemical overall-water-splitting activity. Angew. Chem. Int. Ed. **55**, 6702–6707 (2016)
87. Jayaramulu, K., Masa, J., Tomanec, O., et al.: Nanoporous nitrogen-doped graphene oxide/nickel sulfide composite sheets derived from a metal-organic framework as an efficient electrocatalyst for hydrogen and oxygen evolution. Adv. Funct. Mater. **27**, 1700451 (2017)
88. Ma, W., Ma, R., Wang, C., et al.: A superlattice of alternately stacked Ni–Fe hydroxide nanosheets and graphene for efficient splitting of water. ACS Nano **9**, 1977–1984 (2015)
89. Li, R.-Q., Wang, B.-L., Gao, T., et al.: Monolithic electrode integrated of ultrathin NiFeP on 3D strutted graphene for bifunctionally efficient overall water splitting. Nano Energy **58**, 870–876 (2019)
90. Yuan, Z., Li, J., Yang, M., et al.: Ultrathin black phosphorus-on-nitrogen doped graphene for efficient overall water splitting: dual modulation roles of directional interfacial charge transfer. J. Am. Chem. Soc. **141**, 4972–4979 (2019)
91. Duan, J., Chen, S., Chambers, B.A., et al.: 3D WS_2 nanolayers@heteroatom-doped graphene films as hydrogen evolution catalyst electrodes. Adv. Mater. **27**, 4234–4241 (2015)
92. Duan, J., Chen, S., Jaroniec, M., et al.: Porous C_3N_4 nanolayers@N-graphene films as catalyst electrodes for highly efficient hydrogen evolution. ACS Nano **9**, 931–940 (2015)
93. Elazab, H.A., Siamaki, A.R., Moussa, S., et al.: Highly efficient and magnetically recyclable graphene-supported Pd/Fe_3O_4 nanoparticle catalysts for Suzuki and Heck cross-coupling reactions. Appl. Catal. A **491**, 58–69 (2015)
94. Yan, H., Cheng, H., Yi, H., et al.: Single-atom Pd1/graphene catalyst achieved by atomic layer deposition: remarkable performance in selective hydrogenation of 1,3-butadiene. J. Am. Chem. Soc. **137**, 10484–10487 (2015)
95. Lv, J.-J., Wang, A.-J., Ma, X., et al.: One-pot synthesis of porous Pt–Au nanodendrites supported on reduced graphene oxide nanosheets toward catalytic reduction of 4-nitrophenol. J. Mater. Chem. A **3**, 290–296 (2015)
96. He, K., Chen, G., Zeng, G., et al.: Three-dimensional graphene supported catalysts for organic dyes degradation. Appl. Catal. B **228**, 19–28 (2018)
97. Cheng, Y., Lin, J., Xu, K., et al.: Fischer-Tropsch Synthesis To Lower Olefins Over Potassium-Promoted Reduced Graphene Oxide Supported Iron Catalysts. ACS Catal. **6**, 389–399 (2016)
98. Zhang, L., Hu, J.-S., Huang, X.-H., et al.: Particle-in-box nanostructured materials created via spatially confined pyrolysis as high performance bifunctional catalysts for electrochemical overall water splitting. Nano Energy **48**, 489–499 (2018)
99. Truong, L., Jerng, S.-K., Roy, S.B., et al.: Chrysanthemum-like CoP nanostructures on vertical graphene nanohills as versatile electrocatalysts for water splitting. ACS Sustain. Chem. Eng. **7**, 4625–4630 (2019)
100. Das, D., Santra, S., Nanda, K.K.: In situ fabrication of a nickel/molybdenum carbide-anchored N-doped graphene/CNT hybrid: an efficient (pre) catalyst for OER and HER. ACS Appl. Mater. Interfaces **10**, 35025–35038 (2018)
101. Zhao, Z., Schipper, D.E., Leitner, A.P., et al.: Bifunctional metal phosphide FeMnP films from single source metal organic chemical vapor deposition for efficient overall water splitting. Nano Energy **39**, 444–453 (2017)
102. Liang, H., Jiang, D., Wei, S., et al.: 3D cellular CoS 1.097/nitrogen doped graphene foam: a durable and self-supported bifunctional electrode for overall water splitting. J. Mater. Chem. A **6**, 16235–16245 (2018)
103. Song, H.J., Yoon, H., Ju, B., et al.: 3D architectures of quaternary Co-Ni-S-P/graphene hybrids as highly active and stable

bifunctional electrocatalysts for overall water splitting. Adv. Energy Mater. **8**, 1802319 (2018)
104. Yan, L., Jiang, H., Xing, Y., et al.: Nickel metal–organic framework implanted on graphene and incubated to be ultrasmall nickel phosphide nanocrystals acts as a highly efficient water splitting electrocatalyst. J. Mater. Chem. A **6**, 1682–1691 (2018)
105. Lv, J.J., Zhao, J., Fang, H., et al.: Incorporating nitrogen-doped graphene quantum dots and Ni_3S_2 nanosheets: a synergistic electrocatalyst with highly enhanced activity for overall water splitting. Small **13**, 1700264 (2017)
106. Li, J., Yan, M., Zhou, X., et al.: Mechanistic insights on ternary $Ni_{2-x}Co_xP$ for hydrogen evolution and their hybrids with graphene as highly efficient and robust catalysts for overall water splitting. Adv. Funct. Mater. **26**, 6785–6796 (2016)
107. Zhang, G., Wang, P., Lu, W.-T., et al.: Co nanoparticles/Co, N, S tri-doped graphene templated from in situ-formed Co, S Co-doped g-C_3N_4 as an active bifunctional electrocatalyst for overall water splitting. ACS Appl. Mater. Interfaces **9**, 28566–28576 (2017)
108. Wang, J., Yang, W., Liu, J.: CoP_2 nanoparticles on reduced graphene oxide sheets as a super-efficient bifunctional electrocatalyst for full water splitting. J. Mater. Chem. A **4**, 4686–4690 (2016)
109. Bu, F.-X., Chen, W., Aboud, M.F.A., et al.: Thermal conversion of MOF by microwave: tuning the heterostructure of bimetal phosphide/graphene for highly enhanced electrocatalytic performance. J. Mater. Chem. A **7**, 14526–14535 (2019)
110. Nadeema, A., Walko, P.S., Devi, R.N., et al.: Alkaline water electrolysis by NiZn-double hydroxide-derived porous nickel selenide-nitrogen-doped graphene composite. ACS Appl. Energy Mater. **1**, 5500–5510 (2018)
111. Zhang, W., Ma, X., Zhong, C., et al.: Pyrite-type CoS_2 nanoparticles supported on nitrogen-doped graphene for enhanced water splitting. Front. Chem. **6**, 569 (2018)
112. Dong, T., Zhang, X., Wang, P., et al.: Hierarchical nickel-cobalt phosphide hollow spheres embedded in P-doped reduced graphene oxide towards superior electrochemistry activity. Carbon **149**, 222–233 (2019)
113. Zhuang, M., Liu, Z., Ding, Y., et al.: Methacrylated gelatin-embedded fabrication of 3D graphene-supported Co_3O_4 nanoparticles for water splitting. Nanoscale **11**, 6866–6875 (2019)
114. Tian, J., Chen, J., Liu, J., et al.: Graphene quantum dot engineered nickel-cobalt phosphide as highly efficient bifunctional catalyst for overall water splitting. Nano Energy **48**, 284–291 (2018)
115. Tong, Y., Yu, X., Wang, H., et al.: Trace level Co–N doped graphite foams as high-performance self-standing electrocatalytic electrodes for hydrogen and oxygen evolution. ACS Catal. **8**, 4637–4644 (2018)
116. Liu, Y., Zhu, Y., Shen, J., et al.: CoP nanoparticles anchored on N, P-dual-doped graphene-like carbon as a catalyst for water splitting in non-acidic media. Nanoscale **10**, 2603–2612 (2018)
117. Miao, R., He, J., Sahoo, S., et al.: Reduced graphene oxide supported nickel–manganese–cobalt spinel ternary oxide nanocomposites and their chemically converted sulfide nanocomposites as efficient electrocatalysts for alkaline water splitting. ACS Catal. **7**, 819–832 (2016)
118. Yu, J., Du, Y., Li, Q., et al.: In-situ growth of graphene decorated Ni3S2 pyramids on Ni foam for high-performance overall water splitting. Appl. Surf. Sci. **465**, 772–779 (2019)
119. Huang, H., Yu, C., Yang, J., et al.: Strongly coupled architectures of cobalt phosphide nanoparticles assembled on graphene as bifunctional electrocatalysts for water splitting. ChemElectroChem **3**, 719–725 (2016)
120. Xu, X., Liang, H., Ming, F., et al.: Prussian blue analogues derived penroseite (Ni, Co) Se2 nanocages anchored on 3D graphene aerogel for efficient water splitting. ACS Catal. **7**, 6394–6399 (2017)
121. Hou, Y., Lohe, M.R., Zhang, J., et al.: Vertically oriented cobalt selenide/NiFe layered-double-hydroxide nanosheets supported on exfoliated graphene foil: an efficient 3D electrode for overall water splitting. Energy Environ. Sci. **9**, 478–483 (2016)
122. Cirone, J., Ahmed, S.R., Wood, P.C., et al.: Green synthesis and electrochemical study of cobalt/graphene quantum dots for efficient water splitting. J. Phys. Chem. C **123**, 9183–9191 (2019)
123. Debata, S., Banerjee, S., Sharma, P.K.: Marigold shaped N-rGO-MoS_2-Ni $(OH)_2$ nanocomposite as a bifunctional electrocatalyst for the promotion of overall water splitting in alkaline medium. Electrochim. Acta **303**, 257–267 (2019)
124. Hua, B., Li, M., Zhang, Y.Q., et al.: All-in-one perovskite catalyst: smart controls of architecture and composition toward enhanced oxygen/hydrogen evolution reactions. Adv. Energy Mater. **7**, 1700666 (2017)
125. Liu, G., Zhang, C., Guo, Y., et al.: Enhancing electrocatalytic water splitting activities via photothermal effect over bifunctional nickel/reduced graphene oxide nanosheets. ACS Sustain. Chem. Eng. **7**, 3710–3714 (2019)
126. Debata, S., Patra, S., Banerjee, S., et al.: Controlled hydrothermal synthesis of graphene supported $NiCo_2O_4$ coral-like nanostructures: an efficient electrocatalyst for overall water splitting. Appl. Surf. Sci. **449**, 203–212 (2018)
127. Zhu, Y.P., Guo, C., Zheng, Y., et al.: Surface and interface engineering of noble-metal-free electrocatalysts for efficient energy conversion processes. Acc. Chem. Res. **50**, 915–923 (2017)
128. Jiao, Y., Zheng, Y., Davey, K., et al.: Activity origin and catalyst design principles for electrocatalytic hydrogen evolution on heteroatom-doped graphene. Nat. Energy **1**, 16130 (2016)
129. Agnoli, S., Favaro, M.: Doping graphene with boron: a review of synthesis methods, physicochemical characterization, and emerging applications. J. Mater. Chem. A **4**, 5002–5025 (2016)
130. Liu, L., Yan, F., Li, K., et al.: Ultrasmall $FeNi_3N$ particles with an exposed active (110) surface anchored on nitrogen-doped graphene for multifunctional electrocatalysts. J. Mater. Chem. A **7**, 1083–1091 (2019)
131. Zhang, X., Li, J., Sun, Y., et al.: N-doped reduced graphene oxide supported mixed Ni_2PCoP realize efficient overall water electrolysis. Electrochim. Acta **282**, 626–633 (2018)
132. Hu, Q., Liu, X., Zhu, B., et al.: Crafting MoC_2-doped bimetallic alloy nanoparticles encapsulated within N-doped graphene as roust bifunctional electrocatalysts for overall water splitting. Nano Energy **50**, 212–219 (2018)
133. Hou, Y., Wen, Z., Cui, S., et al.: An advanced nitrogen-doped graphene/cobalt-embedded porous carbon polyhedron hybrid for efficient catalysis of oxygen reduction and water splitting. Adv. Funct. Mater. **25**, 872–882 (2015)
134. Zhang, S., Yu, X., Yan, F., et al.: N-doped graphene-supported Co@CoO core–shell nanoparticles as high-performance bifunctional electrocatalysts for overall water splitting. J. Mater. Chem. A **4**, 12046–12053 (2016)
135. Yang, J., Guo, D., Zhao, S., et al.: Overall water splitting: cobalt phosphides nanocrystals encapsulated by P-doped carbon and married with P-doped graphene for overall water splitting (small 10/2019). Small **15**, 1970052 (2019)
136. Yang, J., Guo, D., Zhao, S., et al.: Cobalt phosphides nanocrystals encapsulated by P-doped carbon and married with P-doped graphene for overall water splitting. Small **15**, 1804546 (2019)
137. Chen, X., Duan, X., Oh, W.-D., et al.: Insights into nitrogen and boron-co-doped graphene toward high-performance peroxymonosulfate activation: maneuverable N–B bonding

configurations and oxidation pathways. Appl. Catal. B **253**, 419–432 (2019)
138. Safardoust-Hojaghan, H., Amiri, O., Hassanpour, M., et al.: S, N co-doped graphene quantum dots-induced ascorbic acid fluorescent sensor: design, characterization and performance. Food Chem. **295**, 530–536 (2019)
139. Chen, W., Xu, L., Tian, Y., et al.: Boron and nitrogen co-doped graphene aerogels: facile preparation, tunable doping contents and bifunctional oxygen electrocatalysis. Carbon **137**, 458–466 (2018)
140. Qu, K., Zheng, Y., Jiao, Y., et al.: Polydopamine-inspired, dual heteroatom-doped carbon nanotubes for highly efficient overall water splitting. Adv. Energy Mater. **7**, 1602068 (2017)
141. Liu, H., Xu, C.-Y., Du, Y., et al.: Ultrathin Co9S8 nanosheets vertically aligned on N, S/rGO for low voltage electrolytic water in alkaline media. Sci. Rep. **9**, 1951 (2019)
142. Zhang, X., Liu, S., Zang, Y., et al.: Co/Co_9S_8@ S, N-doped porous graphene sheets derived from S, N dual organic ligands assembled Co-MOFs as superior electrocatalysts for full water splitting in alkaline media. Nano Energy **30**, 93–102 (2016)
143. Cruz-Silva, E., López-Urías, F., Muñoz-Sandoval, E., et al.: Electronic transport and mechanical properties of phosphorus- and phosphorus–nitrogen-doped carbon nanotubes. ACS Nano **3**, 1913–1921 (2009)
144. Das, D., Nanda, K.K.: One-step, integrated fabrication of Co_2P nanoparticles encapsulated N, P dual-doped CNTs for highly advanced total water splitting. Nano Energy **30**, 303–311 (2016)
145. Hu, Q., Li, G., Li, G., et al.: Trifunctional electrocatalysis on dual-doped graphene nanorings-integrated boxes for efficient water splitting and Zn–air batteries. Adv. Energy Mater. **9**, 1803867 (2019)
146. Liu, M.-R., Hong, Q.-L., Li, Q.-H., et al.: Cobalt boron imidazolate framework derived cobalt nanoparticles encapsulated in B/N codoped nanocarbon as efficient bifunctional electrocatalysts for overall water splitting. Adv. Funct. Mater. **28**, 1801136 (2018)
147. Rao, C.N.R., Gopalakrishnan, K., Govindaraj, A.: Synthesis, properties and applications of graphene doped with boron, nitrogen and other elements. Nano Today **9**, 324–343 (2014)
148. Zhang, X., Ding, P., Sun, Y., et al.: $CoMoS_{3.13}$ nanosheets grafted on B, N co-doped graphene nanotubes as bifunctional catalyst for efficient water electrolysis. J. Alloy. Compd. **731**, 403–410 (2018)
149. Zhou, Y., Gao, G., Li, Y., et al.: Transition-metal single atoms in nitrogen-doped graphenes as efficient active centers for water splitting: a theoretical study. Phys. Chem. Chem. Phys. **21**, 3024–3032 (2019)
150. Zhang, J., Dai, L.: Nitrogen, phosphorus, and fluorine tri-doped graphene as a multifunctional catalyst for self-powered electrochemical water splitting. J Angew. Chem. Int. Ed. **55**, 13296–13300 (2016)

Asad Ali received his master degree (16 year education) with first-class honors in physical chemistry from Department of Chemistry, Gomal University D.I. Khan, Pakistan in 2011 and M.Phil degree in physical chemistry from Department of Chemistry, Islamia College Peshawar, Pakistan in 2017. Currently, he is a Ph.D student under the supervision of Prof. Pei Kang Shen in the Collaborative Innovation Center of Sustainable Energy Materials in Guangxi University, China. His research work focuses on the preparation of graphene-based electrocatalysts and their applications in the fuel cells.

Dr. Pei Kang Shen is a Professor and Director at the Collaborative Innovation Center of Sustainable Energy Materials in Guangxi University, China. Dr. Shen obtained his BSc degree in Electrochemistry at Xiamen University in 1982, and he continuously carried out his research and teaching at the same university for seven years before he became a visiting researcher in the United Kingdom. He received his Ph.D. in Chemistry at Essex University in 1992. From then on he has been working at different universities both in UK, Hong Kong and China. Since 2001, he has been the Professor at the Sun Yat-sen University (Guangzhou, China). He is the author of over 450 publications in qualified journals like *Chem. Rev.*; *Chem. Soc. Rev.*; *J. Am. Chem. Soc.*; *Adv. Mater.*; *Adv. Funct. Mater.*; *Energy Environ. Sci.*; *Adv. Energy Mater.*, *ACS Nano, J. Mater. Chem.*; *J. Power Sources*, including 35 ESI (Highly Cited Papers, 1%) papers and 4 Hot Papers (0.1%) and specialized books (9 in English and Chinese), of 80 patents, and of more than 150 meeting presentations. He is a Highly Cited Scholar in Energy Science in the world for five years (2014-2018). He has organized eight international conferences on Electrochemical Energy Storage and Conversion as a conference Chairman which were promoting the development of electrochemical science in China. He is now working in Guangxi University. He has won the titles of Guangxi Bagui Scholar, National May Day Labor Medal. He pays attention to academic exchanges and cooperation at home and abroad, pays attention to the combination of production, study and research, aims at the needs of the country, and attaches great importance to the industrialization of achievements. A pilot plant with an annual output of 15 tons of graphene has been set up in Nanning High-tech Zone to build the world's first graphene composite asphalt road. His research interests include fuel cells and batteries, electrochemistry of nanomaterials and of nanocomposite functional materials, like graphene powders for different applications and electrochemical engineering. He has also obtained the Second prize in National Natural Science Award of China in 2013 and the First prize in Natural Science Award of Guangdong Province in 2011 and Guangxi Province in 2019.